



Review Article

Recent developments in thermal management of light-emitting diodes (LEDS): A review

Ashish KHUDAIWALA^{1,2,*}, Rupesh L PATEL^{1,3}, Rakesh BUMATARIA²

¹Gujarat Technological University (GTU), Ahmedabad, Gujarat, 382424, India

²Department of Mechanical Engineering, Government Polytechnic, Porbandar, Gujarat, NH-8B, India

³Government Engineering College, Rajkot, Gujarat, 360005, India

ARTICLE INFO

Article history

Received: 30 September 2022

Revised: 07 January 2023

Accepted: 11 January 2023

Keywords:

Life Span; Light Emitting Diode; Heat Pipe; Nanofluid; Thermal Management

ABSTRACT

Light Emitting Diodes (LEDs) is one of the newest ways to light up outdoor areas such as streets, stadiums, airports, military bases, harbors, and high mast towers. The main reason for the high focus is power consumption with better brightness. Even though LEDs have so many benefits, researchers should focus on better managing temperatures as the main reason behind the failure of LEDs is overheating. In this article, modern research trends like using heat pipes filled with nanofluids, ionic winds, spray cooling, use of fins, refrigerants, and oil cooling are focused on and discussed concerning LEDs, solar stills, electric vehicle batteries, and different heat transfer devices to develop a new way to handle the heat from higher-wattage LEDs. There is a research thrust in the field of more than one nanoparticle in the base fluid, and its proportions are not analyzed during LEDs cooling study using a heat pipe. It is necessary to control the heat using a more effective technique. Heat pipe with nanofluid is a more efficient, compact, and cost-effective cooling device to reduce LED failure due to higher heat flux. Hence, it is promising to use nanofluid-filled heat pipes to serve the purpose of the life span enhancement of LEDs.

Cite this article as: Khudaiwala A, Patel RL, Bumataria R. Recent developments in thermal management of light-emitting diodes (LEDS): A review. J Ther Eng 2024;10(2):517–540.

INTRODUCTION

In many application fields, the thermal management of electronic components operating with high heat is a significant issue. The electronic application's constant heat exchange and work recurrence are severe problems for the design of electronic components. Additional heat management from electronic components is required as the electronic structure

is curtailed. The current heat management system needs effective heat transfer using minimized design, particularly for cooling CPUs, LEDs, rectifiers, thyristors, semiconductors, traveling wave gatherers, sound and RF enhancers, and high-thickness semiconductors. It is crucial to enhance cooling since unwavering quality electronic parts are typically reactive to their working temperature.

*Corresponding author.

*E-mail address: khudaiwala_ashish@gtu.edu.in

This paper was recommended for publication in revised form by Editor-in-Chief Ahmet Selim Dalkılıç



LIGHT EMITTING DIODES

Robust state semiconductor devices, the Light Emitting Diodes (LEDs), directly convert electrical energy into visible light. Kim et al. [1], represented that only 10 to 20% of the electrical power in flow-watt-level LEDs is converted to electro-optical energy; the other 80 to 90% is converted to heat. Since the surface area of a LED chip ranges from 1 mm^2 to 2.5 mm^2 , it follows that the hotness dispersing change of an operational LED can achieve 100 W/cm^2 . The intersection temperature of LEDs should be kept under $110 \text{ }^\circ\text{C}$ for better to function correctly and have a long lifespan. Wang et al. [2], concluded that hotness dispersal coefficient should be more significant than $1 \text{ W/cm}^2/^\circ\text{C}$ to provide a convenient expulsion of the hotness created. Since LEDs are hot light sources, heat radiation cannot account for much of how hotness is distributed. The key to effective LED thermal management is to plan an acceptable and skilled heat distribution strategy.

Cooling Devices

Major cooling devices for thermal management A passive device that uses the latent heat of working fluid vaporization to transport heat energy from the heating element

to the cooling element over a relatively long distance. Bumataria et al. [3], divided it in evaporator, adiabatic, and condenser sections comprise of three sub-sections, as shown in Figure 1 and a photocopy of the heat pipe is shown in Figure 2.

Chavda [4], represented that the inner wall of the heat pipe is integrated with multiple structures comprising grooves, sintered powder, wire mesh, and fiber/spring. After achieving the requisite vacuum, the heat pipe is injected with the correct quantity of fluid and sealed. Many varying heat pipe configurations, such as cylinder-shaped heat pipes, flat heat pipes, thermosyphons, pulsating heat pipes, oscillating heat pipes, loop heat pipes, and rotating heat pipes, are seen in the open literature.

Nanofluid

Nanofluids are fluids with nanoparticles of metallic or non-metallic substance uniformly and steadily suspended (less than 100 nm in size). Bumataria et al. [5], concluded that the various nanoparticles in a variety of shapes, like spheroid and cylindrical, are developed by different chemical processes from metallic elements (Ag, Au, Cu, Fe), oxides (Al_2O_3 , CuO, Fe_2O_3 , Fe_3O_4 , MgO, SiO_2 , TiO_2), nitrides (AlN, SiN), carbides (SiC, TiC), and different kinds

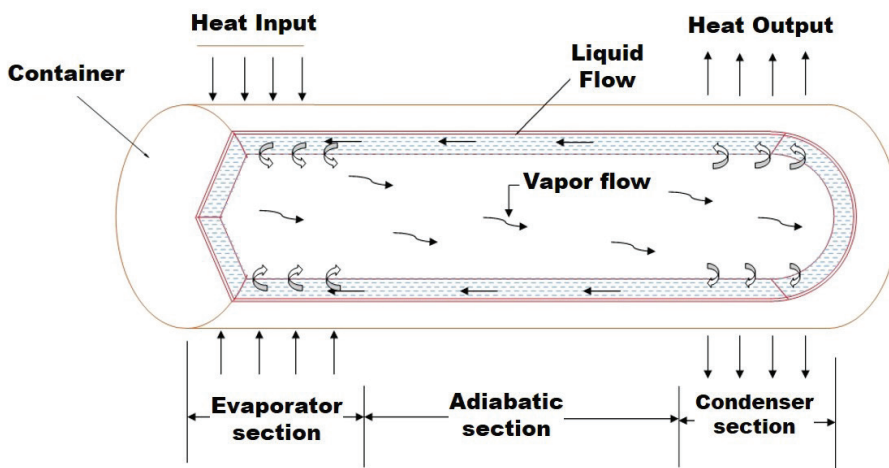


Figure 1. Heat pipe. [From Bumataria et al. [3], with permission from Elsevier.].

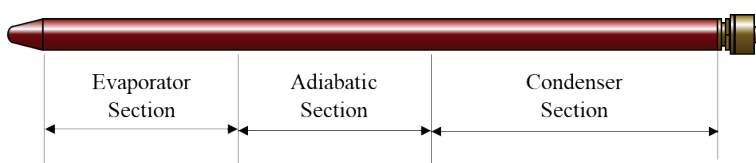


Figure 2. Photocopy of heat pipe.

of carbon (diamond, engine oil, ethylene glycol, graphite, refrigerants, and water are popular base liquids. Chavda et al. [6], concluded that the various base fluids can be combined with nanoparticles in different concentration ratios. Nevertheless, the incorporation of nanoparticles to improve the heat performance of heat pipes is highly dependent on variables such as the nanoparticles' type, size, shape, concentration, and base liquid.

Hybrid Nanofluid

The possibility of enhancing thermal conductivity in single-component nanofluids has been proven in earlier investigations. However, advancement in the study area has been restricted due to the greater desire for superior thermal fluids characteristics. Al_2O_3 , SiO_2 , and TiO_2 are ceramic oxides of reduced thermal conductivity than copper, gold, silver, or carbon compounds. Akilu et al. [7], studied that due to considerably higher mass density, pure metals such as Ag and Cu and oxides such as CuO form more effectively than other oxides such as Al_2O_3 . In recent decades, nanofluids' low thermal conductivity and integrity issues have been rectified by integrating more than one material nano-additives to obtain a synergetic effect, a composite/hybrid nano-additive. The suspending, characterized as a "hybrid nanofluid," incorporates hybrid nano-additives that boost thermal conductivity and stability, promoting the conduction of heat.

Many researchers have been focusing on thermal management to extend the life of electronic components, mainly LEDs, because of how extensively used LEDs are in public and private places. One of the forces influencing the immediate need for development is the untimely failure of LEDs caused by high junction temperatures, which leads to motivation for the thermal management of LEDs with compact, low-cost, and high-performance cooling systems.

To analyze various research trends for thermal management of LEDs, solar stills, electric vehicles, and different heat transfer devices using heat pipes, thermoelectric coolers (TEC), modified heat sinks, ionic wind, fins, and spray cooling, among other devices. The methodology employed for this article contains an introduction related to the essential term, a critical review of the literature, a comparative analysis, a critique outcome of the literature, future scope, and statistical analysis to prove the current scenario. At the paper's end, the literature review recommendations have been drawn as a conclusion.

LITERATURE STUDY

Review of Literature Related to Various Thermal Management Systems Used for Leds

[A] Heat pipe

Kim et al. [8] studied enhancement in heat transfer with nanofluids in a pulsing heat pipe for LED lighting heat dissipation. The experiment's results revealed that a diamond

nanofluid with a 5% convergence increased heat transfer by 18% compared to pure water. Compared to pure water, the Al_2O_3 nanofluid's 0.5% concentration demonstrated a 24% increase in heat transmission rate. Tang et al. [9] investigated high-power LEDs with chips directly attached to heat pipes. They have determined that at 2800 mA, the thermal conductivity of the CHP lead frame is $0.23\text{ }^\circ\text{C/W}$ and $1.65\text{ }^\circ\text{C/W}$. The CHP lead frame LED device's iridescent efficiency is 66.23 m/W at 2800 mA. It is 19.2% more expensive than the standard copper-lead frame. The CHP lead frame's correlated color temperature (CCT) shift value is $108\text{ }^\circ\text{C}$ (381 K), which is 23.5% lower than the copper lead frames. Zheng et al. [10] analyzed a high-power LED lighting system with heat pipe cooling; it was discovered that while cooling with fins, the temperature of the LED substrate reaches $40\text{ }^\circ\text{C}$ in about 5 minutes. However, when using a combination of a fan and heat pipe to cool, the working temperature is just $25\text{ }^\circ\text{C}$. Wang et al. [2] studied High-power LED cooling using a SiO_2 nanofluid screen mesh and wick heat pipe. It was revealed that the thermal resistance of the heat pipe employing SiO_2 nanofluid as the working liquid is 35–40% less than that of purified water at a heat load of 1–60 W heat load. Wang et al. [11] investigated that when the input power was 60 W, and the corresponding maximum LED temperature was maintained below $70\text{ }^\circ\text{C}$, the heat transfer performance of a novel tubular oscillating heat pipe with sintered copper particles inside a flat-plate evaporator and high-power LED heat sink application showed the lowest thermal resistance of 0.168 K/W . Bhullar et al. [12] augmented the thermal performance of a straight heat pipe with an annular screen mesh wick and surfactant-free stable aqueous nanofluids. Using 1 v% of $\text{Al}_2\text{O}_3/\text{DI}$ nanofluids at a low heat input of 12 W, the trial results indicate an ideal reduction of 22 % in the thermal resistance value compared to DI water. Gunnasegaran et al. [13] investigated the Diamond- H_2O nanofluid in the loop heat pipe to transmit heat. According to test results, the thermal resistance of LHP decreased on average by 5.7 wt% to 10.8 wt% when nanoparticle mass concentrations ranged from 0.5 wt% to 3 wt% compared to pure water. Kahani et al. [14] analyzed an artificial neural network, thermal performance of a wick-less heat pipe with $\text{Al}_2\text{O}_3/\text{water}$ nanofluid was predicted. It was established that the percentages of pure water and 3.0 v% $\text{Al}_2\text{O}_3/\text{H}_2\text{O}$ nanofluid with filling ratios of 15, 23, 35, and 45 were 32.3, 24.4, 23.4, and 20, respectively. Chang et al. [15] studied the appropriate thermal control of high-power LEDs; a study studied micro-grooved 3D-printed, flat heat pipes. At a filling ratio of 10%, the highest heat transfer rate and lowest thermal resistance were exhibited. In this manner, the 3D-printed heat pipe was also evaluated in terms of the thermal management of an LED. The LED's lifespan was lengthened, and its temperature was maintained around 40°C . Summary of research work related to heat pipe utilized LED thermal management system is presented and compared in Table 1.

Table 1. Summary of research work related to heat pipe utilized LED thermal management system

Literature	Desc. of Thermal Management System	Desc. of Working Medium	Key Findings	Year
Kim et al. [8]	Pulsating heat pipe	Nanofluid: H ₂ O-based diamond/Al ₂ O ₃ Concentration: 0.5 -5 wt% Particle size: 50 nm	Diamond nanofluid, compared to DI water, showed an 18% increase in heat transfer rate, while Al ₂ O ₃ demonstrated a 24% increase.	2014
Tang et al. [9]	Columnar heat pipe (CHP)	CHP material: Copper Working fluid: ATSM (Water)	The CHP lead structure's thermal resistances R _{l-s} and R _{j-a} are 0.23 °C/W and 1.65 °C/W, respectively, at 2800 mA.	2014
Zheng et al. [10]	Heat pipe and fan	Coolant: demineralized water	LED substrate temperature reaches 400 °C in 5 minutes while cooling by fins at an operating temperature of 25 °C.	2015
Wang et al. [2]	Cylindrical heat pipe	Type of nanofluid: SiO ₂ / water Concentration: 1.0 wt% Particle size:30 nm	At heat loads between 1 and 60 W, the SiO ₂ nanofluid-based heat pipe has a thermal resistance of 35% to 40% lower than that of distilled water.	2016
Wang et al. [11]	Oscillating heat pipe	Type of nanofluid: Cu/Water Concentration: 0.3wt% Particle size: 20 nm	At 60 W heat supply, the thermal resistance of 0.168 K/W was attained. The lowest 70 °C was achieved.	2016
Bhullar et al. [12]	Straight heat pipe	Type of nanofluid: Al ₂ O ₃ /DI water Particle size: 50 nm Concentration: 0-1 wt %	The lowest 22% thermal resistance was obtained at 1 v% and 12 W heat input.	2017
Gunnasegaran et al. [13]	Loop heat pipe	Type of nanofluid: diamond-H ₂ O Concentration: 0-3 wt% Particle size: 50nm	Average 5.7 to 10.8% thermal resistance was obtained at 0.5 to 3 wt%.	2018
Kahani et al. [14]	Wickless heat pipe	Type of nanofluid: Al ₂ O ₃ =/water Concentration: 1-3 wt% Particle size: 10-50 nm	The efficiency enhancement using filling ratios of 15, 23, 35, and 45% were 32.3, 24.4, 23.4, and 20.0, respectively.	2019
Chang et al. [15]	The flat heat pipe, with micro-grooves	Working fluid: acetone filling ratio: 5-50%	A filling ratio of 10% resulted in the most significant rate of heat. The lifespan of the LED was increased, and its temperature was kept at 40 °C.	2021

[B] Modified heat sink

Park et al. [16] studied a hollow cylinder improves the thermal performance of a radial heat sink for LED downlight applications. The results demonstrate that installing an empty chamber improves the heat transfer characteristics of a radial heat sink by up to 43%. Park et al. [17] studied the efficiency and orientation impact of a cross-cut inclined cylindrical heat sink for LED lighting. Thermal resistance was discovered to be the lowest at an inclination angle of 25–30°C for the fins. Park et al. [18], Optimized an LED downlight with a chimney design for radial heat sink cooling effectiveness. It was discovered that the chimney might increase heat sink efficiency by 20% and reduce bulk by 60% compared to a hollow cylinder. Tang et al. [19] studied LED thermal control using a heat sink and vapor chamber. The junction temperatures are consistently below those of the CHS at any current, as shown by temperature-increasing tests.

Additionally, the IHSVC framework's total thermal resistance of junction R_{j-a} is 0.83 °C/W, 16.5% less than the CHS at 3200 mA. Xu et al. [20] investigated heat transmission efficiency for cooling high-power LED lamps using rectangular heat sinks with non-uniform height thermosyphons. The thermal resistance of b- type thermosyphon heat sinks was 8.47–9.91% more in contrast with a- type, whereas type-c has a lower thermal resistance range of 7.26–9.07%. Type-a, type-b, and type-c thermosyphon heat sink, with a temperature threshold of 85 °C, have maximum heat transfer rates of 19 W, 17 W, and 22 W, respectively. Heat transmission efficiency for cooling high-power LED lamps using rectangular heat sinks with non-uniform height thermosyphons. The thermal resistance of type-b thermosyphon heat sinks 8.47–9.91% higher than that of type-a thermosyphon heat sinks, whereas type-c thermosyphon heat sinks have a lower thermal resistance range of 7.26–9.07%. Type-a, type-b, and type-c thermosyphon heat

sink, with a temperature threshold of 85 °C, have maximum heat transfer rates of 19 W, 17 W, and 22 W, respectively. Zu et al. [21] improved heat transmission on a high-emissivity coated passive heat sink. With a heat input of 18 W, the heat sink with and without coating achieved a maximum temperature differential of 26 °C during testing. The findings demonstrated that radiation with layer significantly increased heat exchange and involved 38% of the absolute dispersed power due to the coating's improved heat transfer coefficient of 23% and lowered thermal resistance of 18%. Wang et al. [22] conducted comprehensive studies on the high-power LED street light heat dissipation channel. It has been found that using a printed circuit board with a diamond-like carbon metal center might retard the junction temperature by 17.04 °C. The influence of the street-light surface's hotness dispersion may be improved, and the junction temperature is lowered by 7.04 °C due to the lattice design of the streetlight's shell. The summary of research related to the Modified Heat Sink utilized LED thermal management system is compared and presented in Table 2.

[C] Thermoelectric cooler

Li et al. [23] explored novel uses for a high-power LED automated system. The highest LED power that the automatic cooling system can cool is 106.7 W, while the mechanical cooling system only uses 8.85 W. Xiao et al. [24] investigated a cutting-edge automatic heat-pipe cooling

system for powerful LEDs. According to the simulation (finite element analysis) results, the thermal resistances from the heat sink to the atmosphere and from the LED chip to the atmosphere are 0.373 °C/W, and 5.953 °C/W at 12 W. Lin et al. [25] carried out an experimental investigation. Taguchi analysis of thermoelectric coolers integrated with microchannel heat sinks for LED cooling. Moreover, discovered that, even under difficult operating conditions (Ta: 80 °C, Ti: 55 °C) and modest cooling input (ITEC: 2A, u: 0.49 m/s), the temperature was 60 °C significantly, proving exceptional thermal management execution of the suggested technique. Lin et al. [26] studied the high-power LED's heat transfer properties based on a nanofluid-cooled microchannel heat sink and a thermoelectric cooler. The findings show that replacing water with nanofluids as coolants can reduce temperature up to 18.5 °C and reduce thermal resistance by 42.4%. A 38.6% increase in the MHS heat transfer limit has been made. Sui et al. [27] studied the LED performance increase by an integrated thermoelectric cooling system. The red LED's frequency is reestablished by 5 nm for RGB LEDs cooled by a TEC and a sizable, anticipated heat sink. The illuminance is multiplied by a white LED that is cooled by a TEC with a small, measured heat sink, increasing it from 26768 Lux to 82962 Lux with a TEC power increase from 0-14.4 W. Summary of research work related to Thermoelectric cooler utilized LED thermal management system is compared and presented in Table 3.

Table 2. Summary of research work related to modified heat sink utilized LED thermal management system

Literature	Desc. of Thermal Management System	Desc. of Heat Sink	Key Findings	Year
Park et al. [16]	Radial heat sink	Heat sink: Al alloy 6061 (K: 171 W/m °C) Hollow cylinder: acrylic	Thermal performance was improved by 43%.	2015
Park et al. [17]	Cylindrical heat sink	Heat sink: Al alloy 6061 (K:171 W/moC)	Thermal resistance was discovered to be the lowest at an inclination angle of 25–30°C for the fins.	2016
Park et al. [18]	Radial heat sink	-	The chimney may reduce resistance by 60% while increasing heat sink efficiency by 20%.	2016
Tang et al. [19]	Integrated heat sink with vapor chamber	Vapor chamber: (150 ×150 × 2.8) mm Fins: (150 ×1.6 ×52) mm Numbers fins: 21 Gap fins/mm: 5.4	At 3200 mA, its thermal resistance is 0.83 °C/W, or 16.5% lower than the CHS.	2017
Xu et al. [20]	Rectangular heat sinks with non-uniform height thermosyphons	Working fluid: acetone thermosyphon heat sink: Al alloy	The thermal resistance of the b-type-junction was 8.47–9.91% higher than that of the a-type, whereas the c-type junction has a lower thermal resistance range of 7.26–9.07%.	2021
Zu et al. [21]	Passive heat sink with high-emissivity coating	Coating: carbon materials and SiO ₂	HTC was enhanced by 23%, and thermal resistance was retarded by 18%.	2021
Wang et al. [22]	Heat Dissipation Channel	Street lamp:130W	The junction temperature can be lowered by 7.04 °C while improving the streetlight surface's ability to disseminate heat.	2021

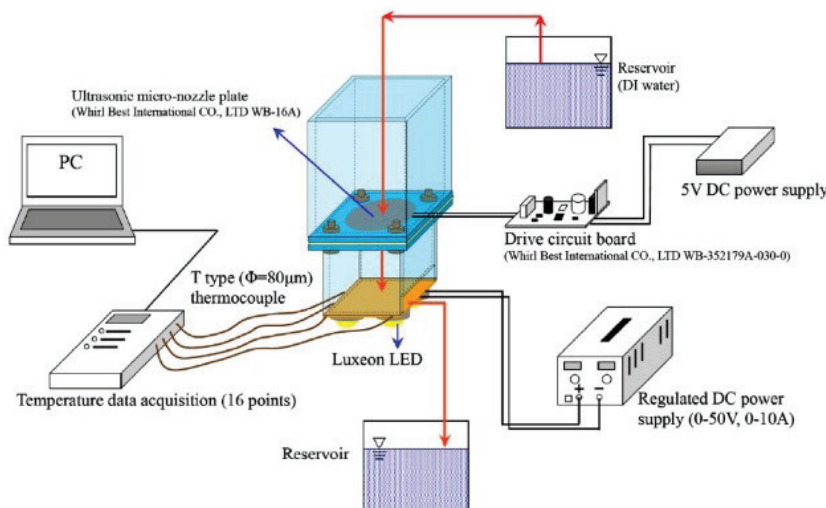
Table 3. Summary of research work related to thermoelectric cooler utilized LED thermal management system

Literature	Desc. of Thermal Management System	Desc. of Thermo-electric Cooler	Key Findings	Year
Li et al. [23]	Thermoelectric cooler, microcontroller, and fan	TEC-K-type thermocouple Microcontroller- MCS-51 Fan-PWM-D07R-12T3U.	The heat reduction in coolant was 106.7 W, while the overall energy consumption was only 8.85 W.	2016
Xiao et al. [24]	Microcontroller, heat pipes, cooling fins, and fan	Microcontroller- MCS-51 Fan- PWM-D07R-12T3U	The simulation findings indicate that the thermal resistances surface to atmosphere and device to the atmosphere are 0.373 °C/W and 5.953 °C/W, respectively, at 12 W.	2017
Lin et al. [25]	Thermoelectric cooler and microchannel heat sink	TEC: TEC1-12706 working fluid: water	Under difficult operating conditions (T_a : 80 °C, T_i : 55 °C) and modest cooling input (ITEC: 2A, u : 0.49 m/s), the LED temperature was shallow at just 60 °C.	2019
Lin et al. [26]	Thermoelectric cooler and a Micro-channel heat sink	Type of nanofluid: TiO ₂ /water Concentration: 0.5 wt% Particle size: 50 nm	Nanofluid can lower the temperature up to 18.5 °C and the thermal resistance by 42.4%. The MHS heat transport limit has been increased by 38.6%.	2020
Sui et al. [27]	Thermoelectric cooler	TEC operating range:0-6V	With TEC power increased from 0W to 14.4 W, the illumination is multiplied from 26,768.93 Lux to 82,962.79 Lux.	2020

[D] Spray cooling

Ye et al. [28] studied a light-emitting diode that is cooled in two phases for greater efficiency and output. The package temperature could remain below 115 °C because of the phase change of the coolant at 2.8 kW LED power. Hsieh et al. [29] created a micro spray-based cooling system for powerful LEDs. Moreover, it was demonstrated that a single spray provides the most significant typical heat transfer coefficient h : 9375 W/m²°C and the least thermal resistance was 2 °C/W between the thermal spreader and the environment. The 3D animation of the experimental setup for LED cooling is presented in Figure 3.

Lay et al.[30], investigated a graphene nano porous layer-based light-emitting diode with efficient micro-spray cooling. A most extreme increase in the illumination of 25% is achieved, and the power rating is increased from 9 W to 12 W. A massive temperature drop of 61.3 °C was observed as a result of improved evaporation. Khandekar et al.[31], studied High-power LED cooling with liquid sprays: problems and potential solutions. The temperature control of high-power LED sources demonstrated a thorough review of flow and heat transport during the impingement of liquid jets on heated surfaces. Cengiz et al. [32] examined heat transfer characteristics of high flux LED and

**Figure 3.** 3D animation of an experimental setup for LED cooling. [From Hsieh et al. [29], with permission from Elsevier.]

concluded that recent findings provide an excellent foundation for intelligent control of phosphor particles to improve the thermal and optical characteristics of both RGB and white LED bundles. Sevilgen et al. [33] experimented with dual-separated cooling channel performance evaluation for high-power led PCB in the vehicle headlight resulted in a temperature reduction of up to 50% on the top copper surface contact with a single LED chip and a 36% reduction in junction temperature. The luminance of the light produced was also increased by about 10%. Gatapova et al. [34] studied a single-phase liquid jet array for controlling the temperature of high-power LED modules. The tests show that substrate-level heat flow may be maintained up to 125 W/cm² while keeping the module surface temperature below 70 °C. Summary of research work related to spray cooling utilized LED thermal management system is compared and presented in Table 4.

[E] Fins

Zhao et al. [35] explained the design and analysis of the thermal model of the high-power LED automobile headlight cooling device. The results show that the heat sink cooling framework's thermal performance is inferior to the heat sink's thermal performance with HCPS. Additionally, 47 mm is the appropriate length for the HCPS. Additionally,

the junction temperature dropped from 116.61 °C to 78.05 °C due to the enforced velocity airflow that was put into place. Huang et al. [36] studied the purpose of removing the heat from powerful automobile LED headlights, and fins with a grooved heat pipe have been designed. The suggested model demonstrated that combining 76 mm-long grooved heat pipes with an effective thermal conductivity of 6000 W/mK and 2 mm-long plate heat dissipation fins on the heat sink with an AlN ceramic having a 180 W/mK proved effective in dissipating heat from high-powered LED headlights within a severely constrained space. Yang et al. [37] focused on developing the thermal conductive composite annular fins to improve the heat transfer of quantum dots in LEDs. The most crucial surface operating temperature of LEDs was found to be 20 °C lower at 1000 mA. The LEDs also displayed a fantastic optical display, boasting a high CRI of 90.3 and a high luminance performance. The summary of research related to fins utilized LED thermal management system is compared and presented in Table 5.

[F] Ionic winds

Wang et al. [38] studied the ionic wind thermal control of high-power light-emitting diodes. When the mesh density was 20 in. and the discharge gap was 5 mm, the ionic wind behaved best; its maximum speed was 1.75 m/s. Shin

Table 4. Summary of research work related to spray cooling utilized LED thermal management system

Literature	Desc. of Thermal Management System	Desc. of Spray Cooling	Key Findings	Year
Ye et al. [28]	Two-phase cooling	Coolant: DI water syringe pump: KDS200	The temperature was able to remain below 115 °C at 2.8 W LED heat.	2013
Hsieh et al. [29]	Micro spray	Working medium- DI water Nozzle diameter: 35 µm Flow rate:0.53 (ml/s)	A single spray's typical heat transfer coefficient (h) is the highest at 9375 W/m ² °C and the lowest at 2 °C/W.	2014
Lay et al. [30]	Micro-spray and GNP coating	Coolant: DI water syringe pump:78-910 °C	At 9 W to 12 W heat input, the temperature retarded by 61.3 °C, and illuminance was enhanced by 25%.	2017
Khandekar et al. [31]	Spray cooling	Orifice dia.:0.594, flow rates:390 ml/min, Reynold Number: 1600 pressure drop: 8 bar	Spray cooling makes better thermal management for high-power LEDs.	2019
Cengiz et al. [32]	Two-Phase Immersion Cooling	Dielectric liquid: Suspended phosphor particles	Findings provide a strong foundation for intelligent control of phosphor particles to improve the thermal and optical characteristics of both RGB and LED bundles.	2020
Sevilgen et al. [33]	Dual-separated cooling channel	Flow rate:0-30 l/min temperature: -20 to120 °C mass flow rate: 0.0002 kg/s to 0.005 kg/s	The temperature plummeted by up to 50% by the time it was over, while the junction temperature dropped by 36%. The luminance of the light produced was also increased by about 10%.	2021
Gatapova et al. [34]	liquid cooling system (Multi-jet single-phase)	Jet dia.:400 µm pressure:0-8 bar flow rates: 65 ml/min to 782 ml/min	According to the results, it may be possible to maintain a substrate-level heat flow of up to 125 W/cm ² while keeping the surface temperature of the module well below 70 °C.	2021

Table 5. Summary of research work related to fins utilized LED thermal management system

Literature	Desc. of Thermal Management System	Desc. of Fins	Key Findings	Year
Zhao et al. [35]	Heat conductive plates (HCPS) and fins	HCPS- Al (6061)	The junction of temperature was retarded from 116.61 °C to 78.05 °C.	2015
Huang et al. [36]	Grooved heat pipe with Fins	Fins: 20 sets Fin spacing: 1.48 mm. coolant: water	The proposed model effectively dissipated heat from LED to the atmosphere.	2019
Yang et al. [37]	Annular Fins.	QDs-AF: 4 fins Thickness:0.28 mm, the mass concentration of hBNs: 15 wt%.	The surface working temperature of LEDs was decreased by 20 °C at 1000 mA. Also, the LEDs demonstrated an incredible optical exhibition with a high CRI of 90.3 and a high luminous performance of 124.1 lm W ⁻¹ .	2021

Table 6. Summary of research work related to ionic winds utilized LED thermal management system

Literature	Desc. of Thermal Management System	Desc. of Ionic Winds	Key Findings	Year
Wang et al. [38]	Ionic wind blower	Ionic wind generator: Wire (d×l): (0.15/0.4 /0.6) ×100 mm Maximum ionic wind velocity was 1.75 m / sec when the mesh density was 20 inches, and the discharge gap was 5 mm. Needle(r×l): (80/480 /1000 μm) × 30 mm Net: 100 × 100 mm	Maximum ionic wind velocity was 1.75 m/s when the mesh density was 20 inches, and the discharge gap was 5 mm.	2017
Shin et al. [39]	Ionic wind	Ionic wind generator: Wire (diameter × length) : (0.5mm/0.4 mm/) × 100 mm The thickness of Fin:5mm	The ionic wind raised the heat transfer coefficient of the heat sink by 37%, from 96.7 to 133 W/m ² K, and boosted its cooling efficacy by 148%.	2018
Bao et al. [40]	Corona Wind by Graphene Decoration	Tungsten steel needles: 80-μm Graphene coating:5-15 μm	The most excellent corona wind speed was around 3 to 4 m / sec, and the case temperature of LED chips was reduced from 64.1 °C to 34.8 °C.	2019

et al. [39] studied that as a result of the thermal flow around the heat sink with ionic wind for high-power LEDs, the heat transfer coefficient of the heat sink increased by 37%, from 96.7 to 133 W/m² K, and the heat sink's cooling performance increased by 148%. Bao et al. [40] experimented with Graphene coating for improved corona wind-based LED heat dissipation. The case temperature of LED chips decreased from 64,1°C to 34,8°C, and the highest corona wind speed reached approximately 3 to 4 m/sec. The summary of research related to ionic winds utilizing LED thermal management systems is compared and presented in Table 6.

[G] Nano paste

Kim et al. [41] experimented with LED cooling performance improvement for an energy conversion application employing nano-paste. The thermal conductivities of CNT

grease and graphene grease were found to increase by up to 16% and 6%, respectively, at 0.75 wt% of the nanoparticles, improving the cooling performance of LED chips by 7.5 °C and 5.5 °C, respectively. Mou et al. [42] enhanced High-power LED heat dissipation using Cu nanoparticle pastes and showed that these LEDs have a low thermal resistance of 6.58 K/W and a specific junction temperature change of 3.22 °C. The summary of research related to Nano Paste utilized LED thermal management system is compared and presented in Table 7.

[H] Miscellaneous

Faranda et al. [43] studied Prototype coolant liquid for LED thermal control. According to the trial findings, the refrigerating fluid lowers the junction temperature and may affect bright radiation displays. Guo et al. [44] analyzed electromagnetic fans for cooling and LED street

Table 7. Summary of research work related to nano paste utilized LED thermal management system

Literature	Desc. of Thermal Management System	Desc. of Working Medium	Key Findings	Year
Kim et al. [41]	Thermal Interface Materials Nano paste made by adding carbon nanotube	Type: MWCNT: Aspect ratio: 650 Graphene: Concentration: 0.25, 0.50, 0.75 wt% Thickness: 0.35 nm	The thermal conductivities of CNT grease and graphene grease increased by 16% and 6%, respectively, at 0.75 wt% of nanoparticles, improving the cooling performance of LED chips by 7.5 °C and 5.5 °C at 0.75 wt% of nanoparticles.	2014
Mou et al. [42]	Nanoparticle Paste	Nanoparticle paste: Cu Particle size (nm): 8	Cu NP paste-packaged LEDs have a low thermal resistance of 6.58 K/W and a standard junction temperature change of 3.21 °C.	2019

Table 8. Summary of research work related to various miscellaneous techniques utilized LED thermal management system

Literature	Desc. of Thermal Management System	Desc. of Technique	Key Findings	Year
Faranda et al. [43]	Refrigerant	Refrigerating Liquid:561 Silicon fluid	Cu NP paste-packaged LEDs have a low thermal resistance of 6.58 K/W and a standard junction temperature change of 3.21 °C.	2012
Guo et al. [44]	Electromagnetic Fans	Fan: 5.44 CFM and 0.5 W	The proposed cooling system can reduce the LEDs’ temperature by 10 °C and increase their lifespan by 2.5 times.	2017
Wu et al. [45]	Diamond-Like Carbon (DLC) films	Thickness of DLC layer (µm): 0 to 3.2 Surface temperature:57 to 60 oC	The experimental results indicate that the surface temperature of LEDs with 1.6, 2.4, and 3.2 pin thick DLC films on an Al substrate is lower by 1.2, 1.5, and 2.3 °C, respectively, than that of LEDs with no DLC film.	2019
Teng et al. [46]	Graphene heat-dissipating coating	Concentration: 0.6 wt %	It was found that illuminance efficacy at Ta of 80 oC is 11.03% and 8.70% higher, and heat dissipation is 6.41% lower for the graphene coating.	2022

lighting. It was discovered that the suggested cooling system might extend the LED lifespan by 2.5 times while lowering the LED temperature by 10°C. Wu et al. [45] analyzed diamond-like carbon coating to improve the high-power LED substrate’s heat radiation. According to the results of the exploratory work, the surface temperatures of LEDs with 1.6, 2.4, and 3.2 pin thick DLC films on the Al substrate are, respectively, 1.2, 1.5, and 2.3°C lower than those of LEDs without DLC films. Teng et al. [46] enhanced the performance of vehicle-LED bulbs utilizing graphene coatings to dissipate heat. Illuminance efficacy was discovered to be 11.03% greater, heat dissipation to be 8.70% higher, and heat dissipation to be 6.41% lower for the graphene covering at an ambient temperature of 80oC. A summary of research on various Miscellaneous Techniques utilized in LED thermal management systems is compared and presented in Table 8.

Review of Literature Related to Various Thermal Systems in Which Heat Pipe Was Used for Thermal Management

[A] Solar still

Saleh et al. [47] experimented with the impact of the solvent during hydrothermal ZnO nanostructure synthesis and solar still application. As a result, rod-shaped nanoparticles outperform sphere-shaped nanoparticles in terms of solar cell productivity by 30%. Rashid et al. [48] studied the improvement of efficiency and output in the nanofluid cascade solar still. The concentration of nanoparticles enhancement by up to 5% determined that hourly fresh-water production is seen at a rate of 22%. Muraleedharan et al. [49], modified Therminol 55-Al₂O₃ nano heat transfer fluid and a Fresnel lens concentrator were used in an active solar distillation system, and it was discovered that 0.1 wt% of nanofluid yielded the highest efficiency. A basin with a 25mm water depth produces the best results. Sahota

et al. [50] studied the thermophysical properties of passive double-slope solar stills loaded with MWCNTs, and Al_2O_3 -water-based nanofluid showed that MWCNTs improved the thermophysical properties of double-sloping solar stills more than Al_2O_3 nanoparticles. The system's primary issue is a performance decline with time. Rafiei et al. [51] studied various nanofluids used in solar desalination systems with a focus point concentrator. The concentration of nanofluids in this system improved freshwater production, and the highest output was attained with a more significant concentration of CuO/oil nanofluid.

Menbari et al. [52] experimentally investigated that the most excellent thermal efficiency of the binary nanofluid-based direct absorption solar parabolic trough collector (DASPTC) was produced by a mixture of 0.2% Al_2O_3 and 0.008% CuO/water hybrid nanofluid. Minea et al. [53] studied recent experimental and numerical comparisons on the effect of hybrid nanofluids on the efficiency of parabolic trough collectors in solar thermal systems. Cu-MgO at a 2 v% concentration produces the highest Nusselt number, and Ag-MgO produces a greater thermal efficiency. Bhalla et al. [54] conducted the experimental investigation of $\text{Al}_2\text{O}_3/\text{CO}_3$ mixed nanoparticles for direct absorption solar thermal collector: photo-thermal study. Results showed that when the concentration of nanofluid increases, so does the weighted absorption of solar radiation. Hybrid nanofluid has a higher photo-thermal efficiency at a 50:50 ratio. Gulzar et al. [55] studied the stability and rheological behavior of hybrid Al_2O_3 - TiO_2 terminal-55 nanofluids in concentrating solar collectors. The hybrid nanofluid's zeta potential value decreases after one week as the concentration increases from 0.05 to 0.5 wt%, going from 54.52 mV to 34.43 mV. Campos et al. [56] experimented with the impact of particle form and graphene oxide on how metal-based nanofluid-utilized direct absorption solar collectors behave under various radiation intensities. At both low and high solar radiation, non-spherical silver nanoparticles and hybrid nanoparticles perform more effectively than spherical silver particles. EI-Gazar et al. [57] prepared energy and exergy analysis for fractional modeling to improve the thermal performance of conventional solar still utilizing a hybrid nanofluid. Energy efficiency has increased by 49.54% in the winter and 23.21% in the summer, respectively.

Mojumder et al. [58] evaluated the performance of an air-type photovoltaic thermal collector system. The fins caused a rise in thermal efficiency from 28.1 to 56.19%. Omidi et al. [59] investigated a humidification-dehumidification desalination system that uses solar collectors and thermoelectric cooling modules. The experimental results show that when the collector air velocity is between 2.2 and 3 m/s and the cost of producing water is kept low, the water output improves by 8%. Khanmohammadi et al. [60] utilized a 3E analysis, and a proposal for a new thermoelectric generator-integrated power-refrigeration system using a parabolic solar collector was created. The system's efficiency is increased by adding a chilled thermoelectric module. Abed

et al. [61] modeled and experimented with a hybrid evaporative cooling system supplemented by an underground heat exchanger and transpired solar collector. This hybrid evaporative cooling system uses less energy by maintaining a room temperature of 2 to 6 °C below the ambient temperature. Yan et al. [62] experimented with a solar still with three effects: immersion cooling and vacuum. According to thermal studies, the heat transfer coefficient of water cooling was 15 to 50 times greater than that of air cooling. Zaite et al. [63] investigated using PV/T collector technology for night radiative cooling; photovoltaic cells perform better. The proposed method allows for the utilization of the annual capacity of the night's radiative uniqueness, which resulted in a savings of 18,49.5 kWh of additional electrical energy each year. Alazwari et al. [64] examined the energy analysis of an air handling unit with a heat recovery unit applied to solar collectors to apply the phase change material. It was discovered that adding phase transition elements to the system reduced its overall irreversibility by roughly 11.6%. Bhagwat et al. [65], experimented performance of a parabolic trough solar collector system supported by finned heat pipes in the climatic conditions of North East India. The average charging efficiency has increased together with the maximum average temperatures for PCM for fins, according to the results. Kateshia et al. [66], carried analysis of Pin fins and phase-change materials are still incorporated into solar panels as absorbent materials. Pin fin using PCM material is a cost-saving choice with a 30% boost in productivity. Summary of research work related to thermal management system of Solar Still is compared and presented in Table 9.

[B] Electric vehicles

Nasir et al. [67] experimented with regulating the temperature of EV lithium-ion batteries via nanofluid-filled heat pipes. $\text{Al}_2\text{O}_3/\text{DI}$ water as the working fluid decreased battery temperature to 4.44 °C and thermal resistance by 15% at 1.5 v%. Chen et al. [68] investigated the thermal management of lithium-ion batteries in electric vehicles, pulsating heat pipes based on nanofluids. The lithium-ion battery's ideal operating temperature for an electric vehicle was discovered to be between 20 and 50 °C. Narayanasamy et al. [69] carried out Looped micro heat pipes with graphene oxide nanofluid for Li-ion batteries: heat transport analysis. Acetone graphene oxide nanofluid with 10 W and 30 W input power produces more significant effects when the filling ratios are 30 and 45%, respectively.

Rani et al. [70] experimented hybrid interface cooling system utilizing nanofluid and air ventilation. Hybrid interface cooling systems perform better than independent cooling systems for battery compartments. Kermani et al. [71] worked on phase change materials embedded in copper foams, and forced-air convection was used in a unique hybrid thermal management system for Li-ion batteries, and it was discovered that the combination of active and passive approaches produced better thermal management

Table 9. Summary of research work related to thermal management system of solar still

Literature	Desc. of Thermal Management System	Desc. of Working Medium	Key Findings	Year
Mono Nanofluids				
Saleh et al. [47]	Half tubular solar still Basin area: 0.18 m ²	ZnO	The result shows that rod shape nanoparticles improve 30% of the productivity of solar still compared to sphere shape nanoparticles	2017
Rashidi et al. [48]	Stepped solar still	Al ₂ O ₃ /water Concentration: 0 to 5 wt%	Hourly production of fresh water is observed at 22% by increasing the concentration of nanoparticles up to 5%	2018
Muraleedharan et al. [49]	single slope solar still Basin area: 1m ²	Al ₂ O ₃ – Therminol-55 Concentration: 0.025, 0.050, 0.075, 0.100 and 0.200 wt%	Maximum efficiency is obtained at 0.1 wt% of nanofluid. A-Basin with a water depth of 25mm gives optimized output.	2019
Sahota et al. [50]	Double slope solar still	Al ₂ O ₃ /water MWCNT/ water Concentration: 0.04, 0.08, and 0.12 wt%	Improvement in thermo-physical property of double slope solar still with MWCNT is higher than Al ₂ O ₃ nanoparticles. The main problem of the system is the degradation of performance with time.	2020
Rafei et al. [51]	Humidification and Dehumidification system with photo voltaic thermal panels	Al ₂ O ₃ /oil, CuO/oil, Cu/oil, TiO ₂ /oil, and MWCNT/oil Concentration: 0 to 5 wt%	Fresh water production is increased with an increase in the concentration of nanofluids, and the highest production is obtained with a higher concentration of CuO/oil nanofluid	2020
Hybrid Nanofluids				
Menbari et al. [52]	Direct absorption solar parabolic trough collector	Al ₂ O ₃ - CuO/water Concentration: 0.05 to 0.2 v%	The highest thermal efficiency of about 48.03% is obtained with a mixture of 0.2 v%, Al ₂ O ₃ -0.008 v%, CuO/water hybrid nanofluid	2016
Minea et al. [53]	parabolic trough collector	Al ₂ O ₃ - Cu, Cu-MgO and Ag-MgO Concentration:0.1 to 2 v%	The highest Nusselt number is obtained with Cu-MgO at 2 v% concentration, and higher thermal efficiency is obtained with Ag-MgO.	2017
Bhalla et al. [54]	Photo-thermal conversion experiment	Al ₂ O ₃ -Cu ₃ O ₄ /DI water Concentration: 0.004 to 0.02 wt%	The weighted absorption of solar energy increases with an increase in nanofluid concentration. The photo-thermal efficiency of a hybrid nanofluid is higher at 50:50 proportions.	2018
Gulzar et al. [55]	Concentrating solar collector	Al ₂ O ₃ -TiO ₂ /Thermino-55 Concentration: 0.05 to 0.5 wt% Proportion: 60:40	The Zeta potential value of hybrid nanofluid decreased from 54.52 mV to 34.43 mV as concentration increased from 0.05 to 0.5 wt% after one week	2019
Campos et al. [56]	Parabolic disc mirror solar collector	Silver, gold, copper, and GO-Silver Concentration: 0.004 and 0.005 v% Proportion: 50:50	The efficiency of non-spherical silver nanoparticles and hybrid nanoparticles is higher than spherical silver particles at low and high solar radiation	2019
EI-Gazar et al. [57]	Single-slope solar still	Al ₂ O ₃ - Cu/water Concentration: 0.05 v% Proportion: 50:50	During the winter and summer, enhancement in the energy efficiency of 49.54% and 23.21% are observed, respectively.	2021
Miscellaneous Techniques				
Mojumder et al. [58]	Fins	Fins- Rectangular working fluid-induced air	Due to fins, the thermal efficiency was hiked by 28.1 to 56.19%.	2016
Omidi et al. [59]	Thermoelectric cooling	Working medium-ethylene glycol	The experimental findings show that between 2.2 and 3 m/s, the collector air velocity increases water output by 8% while maintaining the exact water production costs.	2020
Khanmohammadi et al. [60]	Refrigerated system	Solar collector-parabolic trough	Integrating a refrigerated thermoelectric module into the system improves the exergy performance.	2020

Table 9. Summary of research work related to thermal management system of solar still (continued)

Literature	Desc. of Thermal Management System	Desc. of Working Medium	Key Findings	Year
Abed et al. [61]	Evaporative cooling system	Absorber-Al Plate thickness (mm) 0.7 Porosity 0.005	This hybrid evaporative cooling system conserves electricity by maintaining a room temperature of 2 to 6 °C below the outdoor temperature.	2021
Yan et al. [62]	vacuum and immersion cooling	Absorbing area: 1.09 m ² Vacuum pump: Op. V: 12V; power: 8W Flow rate: 8L/min	Heat transfer testing showed that water cooling was 15-50 times more efficient than air cooling.	2021
Zaite et al. [63]	Radiative cooling	PV/T collector	The proposed method permits the utilization of the annual capacity of the night's radiative uniqueness, saving an additional 18,49 kWh of electrical energy annually.	2021
Alazwari et al. [64]	phase change material	PCM 24 – Gypsum board	It was found that by incorporating phase change materials into the system, the total irreversibility of the system was reduced by almost 11.6%.	2021
Bhagwat et al. [65]	finned heat pipe and PCM	PCM-Paraffin Wax HP working fluid-water HP- Cu Fins-Al	The maximum average temperatures for PCM are higher for fins, along with the increased average charging efficiency.	2021
Kateshia et al. [66]	pin fins and PCM	PCM- Palmitic acid	Pin fin with PCM material is a cost-reducing option with an increased productivity rate of 30%.	2021

outcomes. Kiani et al. [72] investigated a Lithium-ion battery temperature management system with phase-change material and Al₂O₃/AgO/CuO nanofluids. AgO showed the best positive effects and improvements of all the nanoparticles. Wiriyasart et al. [73] studied nanofluid thermal control systems for battery cooling modules in electric vehicles. Suspended nanoparticles significantly improve the battery's cooling capability, and their surface temperature drops by 27.59%. Kiani et al. [74] investigated using a phase-change material, metal foam, and hybrid nanofluid for lithium-ion battery temperature management using hybrid passive cooling. Better battery performance has been observed in performed using this technique. Zhou et al. [75] performed the effectiveness of a hybrid oscillating heat pipe with carbon nanotube nanofluids for cooling the batteries in electric vehicles. A test setup for an EV battery reveals better heat management possibilities. Yetik et al. [76] developed computational modeling of an Al₂O₃-based nanofluid thermal management system for lithium-ion batteries. Following an investigation, it was determined that using air cooling is unsafe for the thermal management of batteries, and the examined nanofluids had tremendous promise as a potential root cause. Kumar et al. [77] experimentally studied an alumina-graphene hybrid nanofluid's thermal and thermo-hydraulic behavior in a small channel heat sink. Heat transfer coefficients are improved using hybrid nanoparticles.

Lyu et al. [78] investigated a thermoelectric cooling system for an electric car's battery. Results of the trials show a promising cooling effect with a reasonable amount of power

dissipation. Sirikasemsuk et al. [79] studied Li-ion battery pack thermal cooling properties with thermoelectric ferrofluid cooling modules. The suggested thermoelectric cooling module displays better cooling performance. Li et al. [80] prepared Herringbone fin-based surrogate model for air-cooling heat dissipation optimization of a battery pack. Herringbone fin and sleeve configuration can enhance battery temperature stability and reduce the adverse effects of air cooling. Huang et al. [81] experimented with the effectiveness of a mini-channel evaporator refrigeration system for power battery thermal management. A mini-channel evaporating refrigeration system is integrated to improve battery thermal control outcomes. Zhao et al. [82] reviewed the battery thermal management systems with air-cooling for electric and hybrid electric cars. With the aid of cutting-edge computational mathematical simulations and contemporary tests, it is shown that air-cooling productivity can be significantly increased by introducing new battery pack concepts, innovative cooling channel designs, and revolutionary thermally conductive materials. The summary of research work related to the thermal management system of Electric is compared and presented in Table 10.

[C] HTD

Yousefi et al. [83] experimented with the effectiveness of CPU coolers considering the use of nanofluids and the impact of heat pipe inclination angle. Moreover, it was discovered that the threshold angle of the heat pipe filled with 0.5 wt% Al₂O₃/water increased thermal resistance. Arya et al. [84] examined the thermal efficiency of a carbon

Table 10. Summary of research work related to thermal management system of electric vehicle

Literature	Desc. of Thermal Management System	Desc. of Working Medium	Key Findings	Year
Mono Nanofluids				
Nasir et al. [67]	Al ₂ O ₃ /DI water-filled heat pipe made aluminum 8mm plate	heat input nanoparticle volume concentration (0.05%, 0.1%, 0.5%, 1.0% and 1.5 v% Al ₂ O ₃)	At 1.5 v%, Al ₂ O ₃ /DI water as working fluid reduced battery temp by 4.44 °C and thermal resistance by 15%	2019
Chen et al. [68]	TiO ₂ /DI water (less than 10 nm) filled closed loop type Pulsating Heat Pipe	The filling ratio of 50%	Excellent heat dissipation efficiency of TMS based on PHP with a TiO ₂ -based NF can reduce the temperature gradient.	2020
Narayansamy et al. [69]	Graphene Oxide filled looped micro heat pipes	filling ratio (15%, 30%, 45%, and 60%) input power	the filling ratio of 30% and 45% provide greater results at 10 W and 30 W input power using Acetone graphene oxide nanofluid	2021
Hybrid Nanofluid				
Rani et al. [70]	Air Ventilation and Nanofluid	Type of nanofluid: Cu + Water and Al ₂ O ₃ + Water Particle size:1 to 100 nm	Hybrid interface cooling systems exhibit better results than individual cooling systems for battery compartments.	2017
Kermani et al. [71]	PCM and forced air convection	PCM: Aluminium	Combined active and passive methods exhibited improved results in thermal management.	2019
Kiani et al. [72]	Nanofluid and PCM	Type of nanofluid: AgO/water Concentration: 2 wt% PCM: Cu foam filled with paraffin wax	Among all the nanoparticles, AgO exhibited the best beneficial and improved results than pure water alone.	2020
Wiriyasart et al. [73]	TiO ₂ /DI water-filled Heat Pipe	Nanoparticle volume concentration (0.25 v%, 0.50 v% of TiO ₂)	Suspended nanoparticles show a significant increase in the cooling capacity of the battery, and their surface temperature decreases by 27.59%.	2020
Kiani et al. [74]	Nanofluid, Metal foam & PCM	Nanofluid: alumina Foam: Copper PCM: paraffin	The hybrid passive cooling combination experimented on in the present study shows excellent cooling results for safe battery operations.	2020
Zhou et al. [75]	Oscillating heat pipe	working fluids: ethanol volumetric filling ratio: 35% volume ratio of water-ethanol mixture: 1:1mass concentration: 0.05 wt% to 0.5 wt%	Experimented setup for EV battery shows provides better options for thermal management.	2021
Yetik et al. [76]	Al ₂ O ₃ nanofluid	Type of nanofluid: Al ₂ O ₃ /water	After analysis, it was concluded that only air cooling is not safe for the thermal management of the batteries, and the nanofluids analyzed showed great potential for the cause.	2021
Kumar et al. [77]	Heat sink	Type of nanofluid: alumina-graphene Concentration: 0.01 v%	Hybrid nanoparticles show improved results for heat transfer coefficients.	2021
Miscellaneous				
Lyu et al. [78]	Thermoelectric cooling	Heater-CSH-02120 Rated power:20 W	The investigations' findings indicate a potential cooling effect with manageable power dissipation.	2019
Sirikasemsuk et al. [79]	Thermoelectric cooling	Coolant: De-ionized water and ferrofluid	The proposed thermoelectric cooling module exhibits better cooling performances	2020

Table 10. Summary of research work related to thermal management system of electric vehicle (continued)

Literature	Desc. of Thermal Management System	Desc. of Working Medium	Key Findings	Year
Li et al. [80]	Herringbone fins	fins thickness: 2.5 mm to 2 mm. Fins angle:15o -17.19o sleeves length changes:12.00 mm to 14.00 mm	The arrangement of herringbone fins and sleeves can enhance the temperature constancy of the battery by reducing the impact of air cooling.	2020
Huang et al. [81]	Refrigeration system	Refrigerant: R134a	Integrating a mini-channel evaporating refrigeration system might boost the battery thermal management results.	2021
Zhao et al. [82]	Air cooling	Design optimization techniques	By introducing new battery pack concepts, innovative cooling channel designs, and novel thermally conductive materials, it is discovered that the efficiency of air-cooling may be significantly boosted using cutting-edge techniques.	2021

nanotube-water nanofluid-cooled flat heat pipe cooling a high heat flux heater. As the mass concentration of the nanofluid grows, the heat pipe's overall thermal resistance decreases. Aprianingsih et al. [85] investigated the electric motor cooling application's thermal performance of pulsing heat pipe. With a minimum thermal resistance of 0.151 °C/W, pulsating heat pipe-filled acetone can reduce the surface temperature of the electric motor (30 W to 150 W) by 55.3 °C. Li et al. [86] studied the SiC-MWCNTs hybrid nanofluids' improved heat transfer efficiency and thermophysical characteristics for automotive radiator systems. With 0.4 v% concentration, hybrid nanofluid's thermal conductivity is increased by 32.01%. Vidhya et al. [87] investigated heat pipe charged with a binary mixture based on ZnO-MgO hybrid nanofluids exhibits thermophysical characteristics and performs well in heat transfer. A more excellent conductivity is attained at 50 °C and 0.1% concentration; the thermal conductivity of hybrid nanofluid increases with temperature and concentration. Xuan et al. [88] conducted ternary hybrid nanofluids' thermo-economic performance and sensitivity analysis. It was discovered that a combination ratio of 40:40:20 produces the highest thermal conductivity. Qomi et al. [89] experimented using a pulsing MHD hybrid nanofluid flow; heat transmission is improved in a microchannel. By including a hybrid nanofluid, the micro-channel heat exchanger's rate of heat transfer is increased.

Bumataria et al. [90] evaluated the performance of the water-based CuO and ZnO hybrid nanofluid-based cylindrical heat pipe. Better performance is obtained with a ratio of 75:25 at a 60° inclination and a heat input range of 60–160 W. Davin et al. [91] studied electric motor oil cooling systems. The cooling performance primarily depends on cooling oil flow rates for temperature reduction. Abdelsalam et.al[92] analyzed heat transfer characteristic of hybrid thermal storage tank and the CFD analysis showed the 85% increase in the charge rate by increasing

the PCM volume fraction from 0.025 to 0.15. Galloni et al. [93] conducted Radial fan CFD analyses for cooling electric motors. According to a CFD study, the fan's flow capacity depends on the impeller's aspect ratio for a given number of blades. Alam et al. [94] numerically studied using micro-pin-fins in a triangle configuration to cool the CPU heat sink. The numerical model suggests that there may be a correlation between higher CPU heat output and more incredible air velocity, as represented by a rise in the Nusselt number. Belarbi et al. [95] conducted an experimental investigation on regulated cooling for the CPU using a thermoelectric and an air-impinging jet. The hybrid cooling solution decreased the temperature of the CPU casing by over 70 °C. Abdulmunem et.al. [96], numerically analysed PV cell temperature regulations with coupled PCM and fins and concluded that use of PCM and fins for PV cell thermal management dropped the temperature for about 14.19%. Pandey et al. [97], carried out BES and CFD analysis for PCM heat exchanger and recommended BES tool for passive use of PCM while co-simulation techniques i.e. BES and CFD is proposed for active use of PCM. Kurhade et al. [98], carried out computational study of PCM cooling for electronic circuit of smart-phone to conclude that the optimum cooling technique proposed in the investigation keeps the temperature of the device below 85°C. Talele et al. [99], experimented PCM based passive battery thermal management system to predict delay effect and found that For 1C rate paraffin wax shows the greater delay time of 11,900s and RT-18 exhibit lower delay time of 10,000s. The summary of research related to the thermal management system of various thermal systems is compared and presented in Table 11.

Critique of Review Work

The results of reported kinds of the literature show the following different types of outcomes:

Table 11. Summary of research work related to thermal management system of various thermal systems

Literature	Desc. of Thermal Management System	Desc. of Working Medium	Key Findings	Year
Yousefi et al. [83]	CPU	Al ₂ O ₃ /DI water Size: < 50nm Angle: 900 to 1800	The Threshold angle of the heat pipe filled with 0.5 wt% Al ₂ O ₃ /water increased thermal resistance.	2013
Arya et al. [84]	High Heat flux heater	CNT/DI water charging ratio: 0.2 and 0.8	As the nanofluid's mass concentration increases, the heat pipe's total thermal resistance lowers.	2017
Prianingsih et al. [85]	Electric motor	pulsating Heat Pipe charging ratio: 0.2 and 0.8 filling ratio:0.5%	With a minimum thermal resistance of 0.151 °C/W, pulsating heat pipe-filled acetone can reduce the surface temperature of the electric motor (30 W to 150 W) by 55.3 °C.	2018
Li et al. [86]	Car radiator	SiC-MWCNT Concentration: 0.04, 0.1, 0.2, and 0.4 v% Proportion: 80:20	The thermal conductivity of hybrid nanofluid is improved by 32.01 v% with 0.4 v% concentration.	2020
Vidhya et al. [87]	Heat pipe	ZnO-MgO Concentration: 0.0125, 0.025, 0.05, 0.075 and 0.1 v% Proportion: 50:50	The thermal conductivity of hybrid nanofluid improves with temperature and concentration; higher conductivity is obtained at 50 °C and 0.1 v% concentration	2020
Xuan et al. [88]	Conductivity measurement using a thermal analyzer	Al ₂ O ₃ -TiO ₂ -Cu/water Concentration: 0.005 to 1 v% Proportion: 20:60:20, 30:50:20, 40:40:20, 50:30:20 and 60:20:20	The highest thermal conductivity is obtained for a mixture ratio of 40:40:20.	2020
Qomi et al. [89]	Micro channel heat exchanger	Type: Cu-Al ₂ O ₃ Concentration: 0.04 v% Proportion: 50:50	The heat transfer rate of the micro-channel heat exchanger is improved by adding hybrid nanofluid	2020
Bumataria et al. [90]	Heat pipe	CuO-ZnO/DI water Concentration: 1 wt% Proportion: 25:75, 50:50 and 75:25	Better performance is obtained with a proportion of 75:25 at 60° inclination and heat input range from 60-160 W	2020
Miscellaneous				
Peng et al. [100]	Fire safety of exterior wall claddings	-	Restricting the instability of protection materials utilized in the outside wall cladding lessens fire mishaps.	2013
Davin et al. [91]	Electric motor	Oil cooling	The cooling performance mainly depends on cooling oil flow rates for temperature reduction.	2015
Abdelsalam et.al. [92]	PCM-heat exchanger	PCM volume fraction: 0.025 to 0.35	CFD analysis shows the 85% increase in the charge rate by increasing the PCM volume fraction from 0.025 to 0.15.	2017
Galloni et al. [93]	Electric motor	Fan	The fan's flow capacity depends on the aspect ratio of the impeller for a particular number of blades, as determined by the CFD study.	2018
Abdulmunem et.al. [96]	PCM-PV cell	PCM: Paraffin wax	Use of PCM and fins for PV cell thermal management dropped the temperature for about 14.19%.	2018
Abdelatif et al. [101]	Elliptic tube Free Convection	Axial distance: 0.1 to 0.9 Inclination: 0-90o Rayleigh Number: 2.6×106 to 2.05×108	At constant Reynold number, the Nu increases with the enhancement in inclination angle	2019

Table 11. Summary of research work related to thermal management system of various thermal systems (continued)

Literature	Desc. of Thermal Management System	Desc. of Working Medium	Key Findings	Year
Abdelatif et al. [102]	Square tube free convection	heat fluxes: 51 W/m ² to 1198 W/m ² Inclination: 0-90°	Nu of 90° increases by 54% more than 0° at 1198 W/m ² .	2019
Alam et al. [94]	CPU	Fins Micro-pin-fin diameter ratio: 0.4 to 0.8	The numerical model shows the possibility of increased heat output from the CPU with enhanced air velocity indicated by an increase in the Nusselt number.	2020
Belarbi et al. [95]	CPU	Thermoelectric cooler and impinging air jet	The hybrid cooling system reduced the CPU case temperature by almost 7 °C.	2020
Pandey et al. [97]	PCM-buildings	PCM heat exchanger: 410* 205* 26 (mm ³)	BES tool is recommended for passive use of PCM while co-simulation techniques i.e BES and CFD is proposed for active use of PCM.	2020
Abdelatif et al. [103]	Semi-circular cylinder with fins	Fin length and thickness	The semi-circular cylinder conveys the best exhibition around an assault point of 15°, while the best exhibition was accomplished utilizing the double fin design.	2021
Kurhade et al. [98]	PCM cooling for smart phone	PCM Thermal Conductivity (W/mK): 0.24	The optimum cooling technique proposed in the investigation keeps the temperature of the device below 85°C.	2021
Talele et.al. [99]	PCM-battery cooling	PCM: Paraffin wax and RT-18	For 1C rate paraffin wax shows the greater delay time of 11,900s and RT-18 exhibit lower delay time of 10,000s	2021

- High-wattage light-emitting diodes are currently the most common choice in lighting applications such as street lights, stadiums, and high mast towers.
- The most well-known methods for LEDs and other electronic components are conventional air cooling, fin cooling, spray cooling, heat pipes, thermoelectric cooling, and ionic winds. Heat pipes were the best alternative when it came to the thermal management of LEDs.
- As proven, using mono & hybrid nanofluids as a working liquid can significantly improve the thermal performance of a heat pipe.
- A limited number of researchers have examined the thermal performance of nanofluid-filled heat pipes to cool electronic components such as electric vehicle batteries, central processing units (CPUs), electric heaters, and LEDs, among other things.
- Numerous studies have been conducted with significant attention to the various types of heat pipes, nanoparticles, base fluids, percentage concentrations, particle sizes, heat pipe orientations, and application types.
- LEDs have complicated and non-linear performance trends, which must be managed via their thermal management.
- Use of PCM in LED cooling might increase fire risk, flame spread, smoke, potential for explosion when held in containers, and liability, it may be wise not to use flammable PCMs for LED cooling at residential or other regularly occupied buildings.
- Apart from electronic component cooling, mono, as well as hybrid nanofluid, can be utilized in automobile radiators [104], solar distillation systems [105], solar collectors, cutting fluid, solar heaters [106], and energy storage systems [107].
The comparative study of works related to LED cooling systems using nanofluid-filled heat pipes is presented in Table 12. The analysis suggests the optimistic hope for thermal management of LED using nanofluid-filled heat pipes due to lower cost, higher heat carrying capacity, and compactness.

Statistical Analysis

This paper examines several thermal management approaches for LEDs and heat pipes as thermal management tools for various electrical devices. Various parts of the review work conducted over the past decade are recognized, including performance characteristics, experimental

Table 12. Comparative study of various work related to LED cooling using nanofluid filled heat pipe

Literature	Types of Heat Pipe	Type of Nanofluid	Output Parameter	Impact
Kim et al. [8]	Pulsating heat pipe	Nanofluid: H ₂ O-based diamond/ Al ₂ O ₃	Heat transfer rate	↑
Tang et al. [9]	Columnar heat pipe (CHP)	CHP material: Copper Working fluid: ATSM (Water)	Thermal resistances	↓
Zheng et al. [10]	Cylindrical heat pipe	Coolant: demineralized water	Operating temperature	↓
Wang et al. [2]	Cylindrical heat pipe	Type of nanofluid: SiO ₂ / water	Thermal resistance	↓
Wang et al. [11]	Oscillating heat pipe	Type of nanofluid: Cu/Water	Thermal resistance	↓
Bhullar et al. [12]	Straight heat pipe	Type of nanofluid: Al ₂ O ₃ /DI water	Thermal resistance	↓
Gunnasegaran et al. [13]	Loop heat pipe	Type of nanofluid: diamond/H ₂ O	Thermal resistance	↓
Kahani et al. [14]	Wickless heat pipe	Type of nanofluid: Al ₂ O ₃ /water	Thermal resistance	↓
Chang et al. [15]	Flat heat pipe	Working fluid: acetone	Junction temperature	↓

analysis, thermal management system description, and working fluids. Significant Elsevier, Taylor & Francis, and Springer publications, as well as a conference proceeding, are the primary sources for the cited works in this article.

The total number of works published in various categories is shown in Figure 4. More research articles on experimental work in heat management systems have been published throughout the previous decade. Due to the non-linear and complex performance tend of the heat pipe, and temperature gradient of LED, the numerical analysis, mathematical model, and CFD work is less in this field. The number of publications between 2012 and 2022 is shown in Figure 5. The trend implies that the research trends have been current and acceding since the last decade. It was concluded that more articles would be produced in 2021.

The number of scholarly articles utilizing specific types of thermal management systems for LEDs is displayed in Figure 6. As indicated in Figure, the most significant number

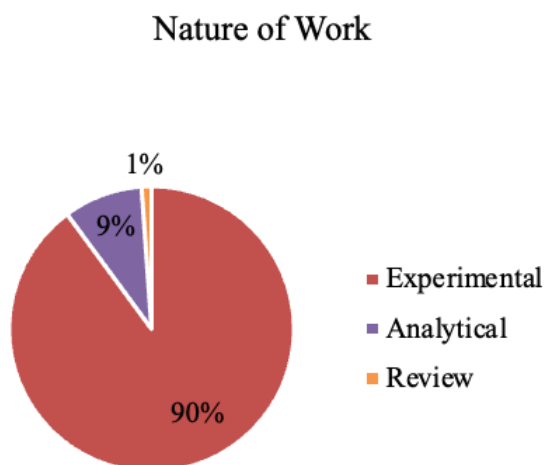


Figure 4. Publications on the nature of work for thermal management systems.

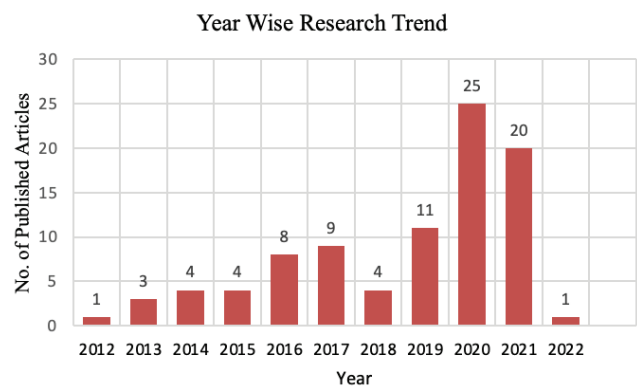


Figure 5. Numbers of publications between 2012 and 2022.

of LED thermal management researchers employed heat pipes and modified heat sinks. The primary usage of heat pipe as a thermal management device shows a favorability as a cooling system due to compactness, high heat carrying capacity, and lower cost.

The number of published research employing heat pipes as a thermal management technique for various thermal devices is demonstrated in Figure 7.

According to the Figure, most researchers used nanofluid-filled heat pipes to control various thermal devices. A recent innovation in thermal management utilizes nanofluid-filled heat pipes. A hybrid nanofluid-filled heat pipe is the most prevalent way to get the synergistic effects of individual nanoparticles nowadays. Current research suggests a nanofluid-filled hybrid hat pipe to regulate thermal devices.

Future Trends

The previous section could be able to forecast where LED thermal management systems stand in terms of research right now. This section discusses a potential line of inquiry toward a new thermal management system for LEDs.

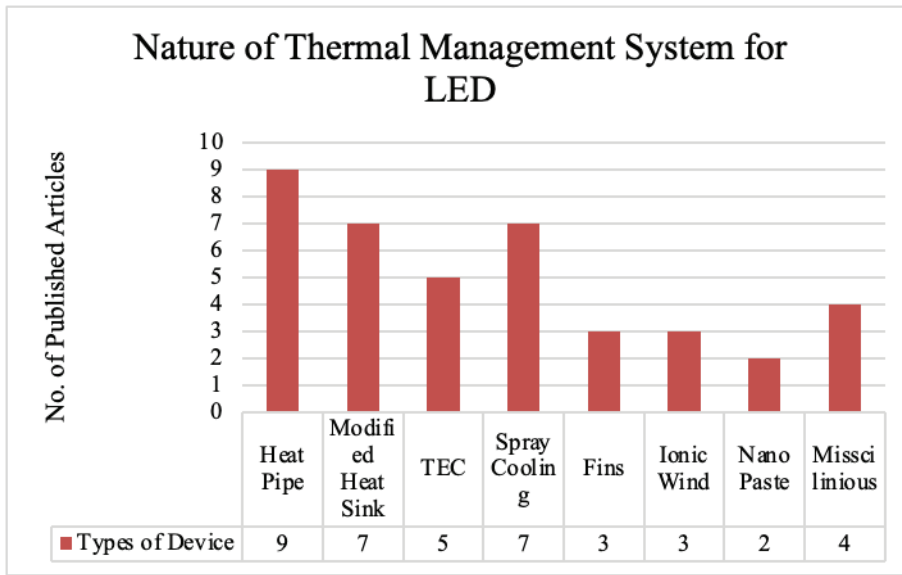


Figure 6. Number of studies and types of thermal management methods for LEDs.

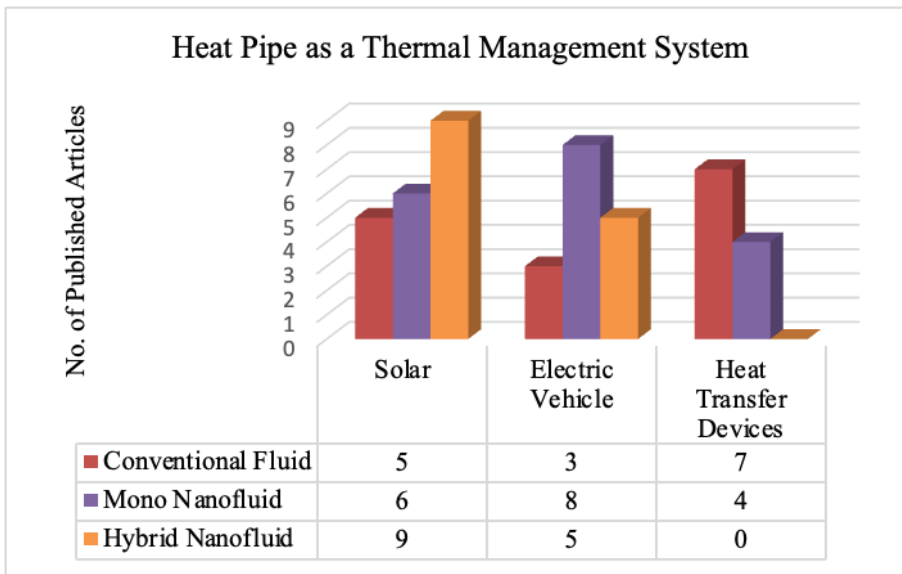


Figure 7. Number of studies as well as working medium types and their application.

Due to their ease of assembly, handling, installation, and low power consumption, LEDs are frequently utilized in commercial and residential applications, including stadiums, high mast towers, and street lights. Substantial research has been done on nanofluid-filled heat pipes for the thermal control of LEDs. The change in LED performance for changing heat loads, ideal orientation, and application types using heat pipes as a thermal management system can be the subject of future research.

As a working medium-filled heat pipe, traditional mono nanofluid has been the subject of much research for the thermal management of heat transfer devices. Particularly for

practical applications such as LEDs cooling, there has been little research on the application of hybrid nanofluid and the comparison of hybrid nanofluid to nanofluid wherein individual nanoparticles was suspended. The published research works pertain to nanofluid types, wick structure types, nanoparticle concentration, filling ratio, orientation, and heat load. When applied in actual applications, hybrid nanofluids might be used to undertake an extensive study into the effect of varied, suspended nanoparticles, suspended particle, percentage concentration, filling ratio, surface shape, and preparation method on the thermal performance of heat pipes.

The thermal management of heat transfer devices has been the subject of much research utilizing a heat pipe filled with mono nanofluid as a working medium. Particularly for practical applications such as LED cooling, there has been limited research on the usage of hybrid nanofluid and the comparison of hybrid nanofluid to nanofluid in which individual nanoparticles were suspended. The published research addresses many topics, including nanofluid types, wick structure types, nanoparticle concentration, filling ratio, orientation, and heat load. Using hybrid nanofluids, researchers can examine the effect of different suspended nanoparticles, their proportion, concentration, filling ratio, surface shape, and preparation technique on the thermal performance of heat pipes, especially for practical applications.

CONCLUSION

This paper explored the thermal management of LEDs and heat pipes as a thermal management system for thermal devices employing nanofluids, both mono, and hybrid, as a medium for work. Open literature indicates that mono and hybrid nanofluid-filled heat pipes have excellent promise for LED thermal management. From the study, the following findings can be drawn:

1. High-wattage LEDs are now most prevalent in lighting applications like Street lights, Stadiums, and High mast towers. Reducing LED's life span due to the overheating problem needs attention.
2. There is a scope to design and test a cooling system of high-wattage LEDs for life span enhancement.
3. Cooling curves needed to be compared for various applications of the LEDs.
4. Limited researchers have used a combination of more than one nanoparticle in base fluid with various proportions to investigate the heat pipe for actual life application.
5. Due to the complex and non-linear performance trend of LED cooling, experimental work is needed to be carried out for the thermal management of LEDs.
6. Increased heat transfer at the evaporator section of a heat pipe made of nanofluids may result from (1) bombardments of suspended nanoparticles that create more vapor bubbles and reduce their size and number, (2) improvements in the thermophysical properties of the working medium, such as thermal conductivities, and (3) an artificial layer of nanoparticles on the surface of the wall that increases the heat transfer coefficient and heat flux. As a result of the deposition of nanoparticles on the surface, a porous structure is created, which increases the surface area for heat transfer.
7. Adopting a working medium composed of hybrid nanoparticles is essential to enhance heat transfer rate and stability while decreasing viscosity due to the synergistic impact.

In addition, theoretical and experimental research is required to comprehend the thermal management of LEDs employing hybrid nanofluid-filled heat pipes for diverse applications such as street lights, stadiums, and high mast towers.

NOMENCLATURE

Abbreviations

Ag	Silver
Al ₂ O ₃	Aluminium Oxide
AlN	Aluminum Nitride
Au	Gold
CCT	Correlated Colour Temperature
CHP	Closed Loop Heat Pipe
CHS	Conventional Heat Sink
CNT	Carbon Nanotube
CPU	Central Processing Unit
CRI	Colour Rendering Index
Cu	Copper
CuO	Copper Oxide
DASPTC	Direct Absorption Solar Trough Collector
DLC	Diamond-Like Carbon
EV	Electric Vehicle
Fe ₂ O ₃ /Fe ₃ O ₄	Iron Oxide
HCPS	Heat Conductive Plates
IHSVC	Integrated Heat Sink with Vapour Chamber
LED	Light Emitting Diode
LHP	Loop Heat Pipe
MgO	Magnesium Oxide
MHS	Micro-channel Heat Sink
MWCNT	Multi-Wall Carbon Nanotube
NP	Nano Particles
PCM	Phase Change Material
PHP	Pulsating Heat Pipe
SiC	Silicon Carbide
SiN	Silicon Nitride
SIN	Silicon Nitride
SiO ₂	Silicon Oxide
TEC	Thermo-Electric Cooler
TiC	Tungsten Carbide
TiO ₂	Titanium Oxide
TMS	Thermal Management System

Symbol

HTC	Heat Transfer Coefficient (W/mK)
T	Temperature (°C)
v	Volume Fraction (%)
wt	Weight Fraction (%)

Subscripts

A	Ambient
---	---------

AUTHORSHIP CONTRIBUTIONS

Authors equally contributed to this work.

DATA AVAILABILITY STATEMENT

The authors confirm that the data that supports the findings of this study are available within the article. Raw data that support the finding of this study are available from the corresponding author, upon reasonable request.

CONFLICT OF INTEREST

The author declared no potential conflicts of interest with respect to the research, authorship, and/or publication of this article.

ETHICS

There are no ethical issues with the publication of this manuscript.

REFERENCES

- [1] Kim D, Lee J, Kim J, Choi CH, Chung W. Enhancement of heat dissipation of LED module with cupric-oxide composite coating on aluminum-alloy heat sink. *Energy Convers Manag* 2015;106:958–963. [\[CrossRef\]](#)
- [2] Wang Y, Zhang J, Cen J, Jiang F. A feasibility study about using SiO₂ nanofluid screen mesh wick heat pipe for cooling of high-power LEDs. *Heat Transf Eng* 2016;37:741–750. [\[CrossRef\]](#)
- [3] Bumataria RK, Chavda NK, Panchal H, Nalbandh AH. Current research aspects in mono and hybrid nanofluid based heat pipe technologies. *Heliyon* 2019;00:1–16. [\[CrossRef\]](#)
- [4] Chvda NK. Review of Modeling the performance of heat pipes using artificial neural network. 2017;7:7–12.
- [5] Bumataria R, Chavda N. Heat load and orientation impacts in cylindrical heat pipes using copper oxide, aluminium oxide, and zinc oxide nanofluids. *Int J Ambient Energy* 2021;43:1–20. [\[CrossRef\]](#)
- [6] Chavda N, Bumataria R. Effect of particle size and concentration on thermal performance of cylindrical shaped heat pipe using silver-DI water nanofluid. *Int J Ambient Energy* 2022;43:1–20. [\[CrossRef\]](#)
- [7] Akilu S, Tesfamichael A, Azman M, Said M, Adriana A. Solar energy materials and solar cells properties of glycerol and ethylene glycol mixture based SiO₂-CuO/C hybrid nanofluid for enhanced solar energy transport. *Sol Energy Mater Sol Cells* 2017. [\[CrossRef\]](#)
- [8] Kim HT, Bang KH. Heat transfer enhancement of nanofluids in a pulsating heat pipe for heat dissipation of LED lighting. *J Korean Soc Mar Eng* 2014;38:1200–1205. [\[CrossRef\]](#)
- [9] Tang Y, Ding X, Yu B, Li Z, Liu B. A high power LED device with chips directly mounted on heat pipes. *Appl Therm Eng* 2014;66:632–639. [\[CrossRef\]](#)
- [10] Zheng J, Ge D, Li J. The analysis of heat pipe cooling in high power LED lighting system. 16th Int Conf Electron Packag Technol ICEPT 2015:480–482. [\[CrossRef\]](#)
- [11] Wang H, Qu J, Peng Y, Sun Q. Heat transfer performance of a novel tubular oscillating heat pipe with sintered copper particles inside flat-plate evaporator and high-power LED heat sink application. *Energy Convers Manag* 2019;189:215–222. [\[CrossRef\]](#)
- [12] Bhullar BS, Gangacharyulu D, Das SK. Augmented thermal performance of straight heat pipe employing annular screen mesh wick and surfactant free stable aqueous nanofluids. *Heat Transf Eng* 2017;38:217–226. [\[CrossRef\]](#)
- [13] Gunnasegaran P, Abdullah MZ, Yusoff MZ, Kanna R. Heat transfer in a loop heat pipe using diamond-H₂O nanofluid. *Heat Transf Eng* 2018;39:1117–1131. [\[CrossRef\]](#)
- [14] Kahani M, Vatankhah G. Thermal performance prediction of wickless heat pipe with Al₂O₃/water nanofluid using artificial neural network. *Chem Eng Commun* 2019;206:509–523. [\[CrossRef\]](#)
- [15] Chang C, Han Z, He X, Wang Z, Ji Y. 3D printed aluminum flat heat pipes with micro grooves for efficient thermal management of high power LEDs. *Sci Rep* 2021;11:1–8. [\[CrossRef\]](#)
- [16] Park SJ, Jang D, Lee KS. Thermal performance improvement of a radial heat sink with a hollow cylinder for LED downlight applications. *Int J Heat Mass Transf* 2015;89:1184–1189. [\[CrossRef\]](#)
- [17] Park SJ, Jang D, Lee KS. Thermal performance and orientation effect of an inclined cross-cut cylindrical heat sink for LED light bulbs. *Int J Heat Mass Transf* 2016;103:1371–1377. [\[CrossRef\]](#)
- [18] Park SJ, Jang D, Yook SJ, Lee KS. Optimization of a chimney design for cooling efficiency of a radial heat sink in a LED downlight. *Energy Convers Manag* 2016;114:180–187. [\[CrossRef\]](#)
- [19] Tang Y, Lin L, Zhang S, Zeng J, Tang K, Chen G, et al. Thermal management of high-power LEDs based on integrated heat sink with vapor chamber. *Energy Convers Manag* 2017;151:1–10. [\[CrossRef\]](#)
- [20] Xu Z. Heat transfer performance of the rectangular heat sinks with non-uniform height thermosyphons for high power LED lamps cooling. *Case Stud Therm Eng* 2021;25. [\[CrossRef\]](#)
- [21] Zu H, Dai W, Li Y, Li K, Li J. Analysis of enhanced heat transfer on a passive heat sink with high-emissivity coating. *Int J Therm Sci* 2021;166. [\[CrossRef\]](#)
- [22] Wang Z, Bao Q, Li Y, Zou J, Zheng H, Yang J, et al. Systematic research on the heat dissipation channel of high power LED street lamps. *J Phys Conf Ser* 2021;1952. [\[CrossRef\]](#)
- [23] Li J, Zhang X, Zhou C, Zheng J, Ge D, Zhu W. New applications of an automated system for high-power LEDs. *IEEE/ASME Trans Mechatronics* 2016;21:1035–1042. [\[CrossRef\]](#)

- [24] Xiao C, Liao H, Wang Y, Li J, Zhu W. A novel automated heat-pipe cooling device for high-power LEDs. *Appl Therm Eng* 2017;111:1320–1329. [CrossRef]
- [25] Lin X, Mo S, Jia L, Yang Z, Chen Y, Cheng Z. Experimental study and Taguchi analysis on LED cooling by thermoelectric cooler integrated with micro-channel heat sink. *Appl Energy* 2019;242:232–238. [CrossRef]
- [26] Lin X, Mo S, Mo B, Jia L, Chen Y, Cheng Z. Thermal management of high-power LED based on thermoelectric cooler and nanofluid-cooled microchannel heat sink. *Appl Therm Eng* 2020;172. [CrossRef]
- [27] Sui G, Chen J, Ni H, Ma Y, Gao X, Wang N. Improvement of LED performance with an integrated thermoelectric cooling package. *IEEE Access* 2020;8:116535–116543. [CrossRef]
- [28] Ye H, Mihailovic M, Wong CKY, van Zeijl HW, Gielen AWJ, Zhang GQ, et al. Two-phase cooling of light emitting diode for higher light output and increased efficiency. *Appl Therm Eng* 2013;52:353–359. [CrossRef]
- [29] Hsieh SS, Hsu YF, Wang ML. A microspray-based cooling system for high powered LEDs. *Energy Convers Manag* 2014;78:338–346. [CrossRef]
- [30] Lay KK, Cheong BMY, Tong WL, Tan MK, Hung YM. Effective micro-spray cooling for light-emitting diode with graphene nanoporous layers. *Nanotechnology* 2017;28:164003. [CrossRef]
- [31] Khandekar S, Sahu G, Muralidhar K, Gatapova EY, Kabov OA, Hu R, et al. Cooling of high-power LEDs by liquid sprays: Challenges and prospects. *Appl Therm Eng* 2021;184:115640. [CrossRef]
- [32] Cengiz C, Muslu AM, Arik M, Dogruoz B. Enhanced thermal performance of high flux LED systems with two-phase immersion cooling. *Intersoc Conf Therm Thermomechanical Phenom Electron Syst* 2020-July. [CrossRef]
- [33] Sevilgen G, Kilic M, Aktas M. Dual-separated cooling channel performance evaluation for high-power led Pcb in automotive headlight. *Case Stud Therm Eng* 2021;25. [CrossRef]
- [34] Gatapova EY, Sahu G, Khandekar S, Hu R. Thermal management of high-power LED module with single-phase liquid jet array. *Appl Therm Eng* 2021;184:116270. [CrossRef]
- [35] Zhao XJ, Cai YX, Wang J, Li XH, Zhang C. Thermal model design and analysis of the high-power LED automotive headlight cooling device. *Appl Therm Eng* 2015;75:248–258. [CrossRef]
- [36] Huang DS, Chen TC, Tsai LT, Lin MT. Design of fins with a grooved heat pipe for dissipation of heat from high-powered automotive LED headlights. *Energy Convers Manag* 2019;180:550–558. [CrossRef]
- [37] Yang X, Zhou S, Xie B, Yu X, Zhang X, Xiang L, et al. Enhancing heat dissipation of quantum dots in high-power white LEDs by thermally conductive composites annular fins. *IEEE Electron Device Lett* 2021;42:1204–1207. [CrossRef]
- [38] Wang J, Cai YX, Li XH, Zhao XD, Wang J, Shi YF, et al. Experimental investigation of high-power light-emitting diodes' thermal management by ionic wind. *Appl Therm Eng*. 2017;122:49–58. [CrossRef]
- [39] Shin DH, Sohn DK, Ko HS. Analysis of thermal flow around heat sink with ionic wind for high-power LED. *Appl Therm Eng* 2018;143:376–384. [CrossRef]
- [40] Bao YC, Cai YX, Wang J, Shi YF, Wang JB. Experimental study on LED heat dissipation based on enhanced corona wind by graphene decoration. *IEEE Trans Plasma Sci* 2019;47:4121–4126. [CrossRef]
- [41] Kim CM, Kang YT. Cooling performance enhancement of LED (Light Emitting Diode) using nanopastes for energy conversion application. *Energy* 2014;76:468–476. [CrossRef]
- [42] Mou Y, Wang H, Peng Y, Cheng H, Sun Q, Chen M. Enhanced heat dissipation of high-power light-emitting diodes by Cu nanoparticle paste. *IEEE Electron Device Lett* 2019;40:949–952. [CrossRef]
- [43] Faranda R, Guzzetti S, Lazaroiu GC, Leva S. Refrigerating liquid prototype for LED's thermal management. *Appl Therm Eng* 2012;48:155–163. [CrossRef]
- [44] Guo ZL, Su HC, Xu HY. Analysis on LED street lamp cooling using electromagnetic fans. *Annu IEEE Semicond Therm Meas Manag Symp* 2017;18:278–282. [CrossRef]
- [45] Wu X, Duan W, Wu S, Zhang J. Analysis of diamond-like carbon film on enhancing thermal radiation of substrate of high-power LED. *2019 20th Int Conf Electron Packag Technol ICEPT* 2019:5–8. [CrossRef]
- [46] Teng TP, Chen WJ, Chang CH. Enhanced heat dissipation performance of automotive led lamps using graphene coatings. *Polymers (Basel)* 2022;14. [CrossRef]
- [47] Saleh SM, Soliman AM, Sharaf MA, Kale V, Gadgil B. Influence of solvent in the synthesis of nano-structured ZnO by hydrothermal method and their application in solar-still. *J Environ Chem Eng* 2017;5:1219–1226. [CrossRef]
- [48] Rashidi S, Bovand M, Rahbar N, Esfahani JA. Steps optimization and productivity enhancement in a nanofluid cascade solar still. *Renew Energy* 2018;118:536–545. [CrossRef]
- [49] Muraleedharan M, Singh H, Udayakumar M, Suresh S. Modified active solar distillation system employing directly absorbing Therminol 55-Al₂O₃ nano heat transfer fluid and Fresnel lens concentrator. *Desalination* 2019;457:32–38. [CrossRef]
- [50] Sahota L, Arora S, Singh HP, Sahoo G. Thermophysical characteristics of passive double slope solar still loaded with mwcnts and al₂o₃-water based nanofluid. *Mater Today Proc* 2019;32:344–349. [CrossRef]

- [51] Rafiei A, Loni R, Mahadzir SB, Najafi G, Pavlovic S, Bellos E. Solar desalination system with a focal point concentrator using different nanofluids. *Appl Therm Eng* 2020;174:115058. [\[CrossRef\]](#)
- [52] Menbari A, Alemrajabi AA, Rezaei A. Experimental investigation of thermal performance for direct absorption solar parabolic trough collector (DASPTC) based on binary nanofluids. *Exp Therm Fluid Sci* 2017;80:218–227. [\[CrossRef\]](#)
- [53] Minea AA, El-Maghlany WM. Influence of hybrid nanofluids on the performance of parabolic trough collectors in solar thermal systems: Recent findings and numerical comparison. *Renew Energy* 2018;120:350–364. [\[CrossRef\]](#)
- [54] Bhalla V, Khullar V, Tyagi H. Experimental investigation of photo-thermal analysis of blended nanoparticles (Al₂O₃/Co₃O₄) for direct absorption solar thermal collector. *Renew Energy* 2018;123:616–626. [\[CrossRef\]](#)
- [55] Gulzar O, Qayoum A, Gupta R. Experimental study on stability and rheological behaviour of hybrid Al₂O₃-TiO₂ Therminol-55 nanofluids for concentrating solar collectors. *Powder Technol* 2019;352:436–444. [\[CrossRef\]](#)
- [56] Campos C, Vasco D, Angulo C, Burdiles PA, Cardemil J, Palza H. About the relevance of particle shape and graphene oxide on the behavior of direct absorption solar collectors using metal based nanofluids under different radiation intensities. *Energy Convers Manag* 2019;181:247–257. [\[CrossRef\]](#)
- [57] El-Gazar EF, Zahra WK, Hassan H, Rabia SI. Fractional modeling for enhancing the thermal performance of conventional solar still using hybrid nanofluid: Energy and exergy analysis. *Desalination* 2021;503:114847. [\[CrossRef\]](#)
- [58] Mojumder JC, Chong WT, Ong HC, Leong KY, Abdullah-Al-Mamoon. An experimental investigation on performance analysis of air type photovoltaic thermal collector system integrated with cooling fins design. *Energy Build* 2016;130:272–285. [\[CrossRef\]](#)
- [59] Omidi B, Rahbar N, Kargarsharifabad H, Rashidi S. Combination of a solar collector and thermoelectric cooling modules in a humidification-dehumidification desalination system-experimental investigation with energy, exergy, exergoeconomic and environmental analysis. *Energy Convers Manag* 2020;225. [\[CrossRef\]](#)
- [60] Khanmohammadi S, Musharavati F, Kizilkan O, Duc Nguyen D. Proposal of a new parabolic solar collector assisted power-refrigeration system integrated with thermoelectric generator using 3E analyses: Energy, exergy, and exergo-economic. *Energy Convers Manag* 2020;220:113055. [\[CrossRef\]](#)
- [61] Abed FM, Zaidan MH, Hasanuzzaman M, Kumar L, Jasim AK. Modelling and experimental performance investigation of a transpired solar collector and underground heat exchanger assisted hybrid evaporative cooling system. *J Build Eng* 2021;44:102620. [\[CrossRef\]](#)
- [62] Yan T, Xie G, Chen W, Wu Z, Xu J, Liu Y. Experimental study on three-effect tubular solar still under vacuum and immersion cooling. *Desalination* 2021;515:115211. [\[CrossRef\]](#)
- [63] Zaitte A, Belouaggadia N, Abid C, Ezzine M. Performance improvement of photovoltaic cells using night radiative cooling technology in a PV/T collector. *J Build Eng* 2021;42:102843. [\[CrossRef\]](#)
- [64] Alazwari MA, Abu-Hamdeh NH, Khoshaim A, Ashour AI, Nusier OK, Karimipour A. Effects of examine the phase change material through applying the solar collectors: exergy analysis of an air handling unit equipped with the heat recovery unit. *J Energy Storage* 2021;41:103002. [\[CrossRef\]](#)
- [65] Bhagwat VV, Roy S, Das B, Shah N, Chowdhury A. Performance of finned heat pipe assisted parabolic trough solar collector system under the climatic condition of North East India. *Sustain Energy Technol Assess* 2021;45:101171. [\[CrossRef\]](#)
- [66] Kateshia J, Lakhera VJ. Analysis of solar still integrated with phase change material and pin fins as absorbing material. *J Energy Storage* 2021;35:102292. [\[CrossRef\]](#)
- [67] Nasir FM, Abdullah MZ, Majid MFMA, Ismail MA. Nanofluid-filled heat pipes in managing the temperature of EV lithium-ion batteries. *J Phys Conf Ser* 2019;1349:012123. [\[CrossRef\]](#)
- [68] Chen M, Li J. Nanofluid-based pulsating heat pipe for thermal management of lithium-ion batteries for electric vehicles. *J Energy Storage* 2020;32:101715. [\[CrossRef\]](#)
- [69] Narayanasamy MP, Gurusamy S, Sivan S, Senthilkumar AP. Heat transfer analysis of looped micro heat pipes with graphene oxide nanofluid for Li-Ion battery. *Therm Sci* 2021;25:395–405. [\[CrossRef\]](#)
- [70] Rani MFH, Razlan ZM, Bakar SA, Desa H, Wan WK, Ibrahim I, et al. Experimental study of hybrid interface cooling system using air ventilation and nanofluid. *AIP Conf Proc* 2017;1885:020073. [\[CrossRef\]](#)
- [71] Mehrabi-Kermani M, Houshfar E, Ashjaee M. A novel hybrid thermal management for Li-ion batteries using phase change materials embedded in copper foams combined with forced-air convection. *Int J Therm Sci* 2019;141:47–61. [\[CrossRef\]](#)
- [72] Kiani M, Omiddezyani S, Houshfar E, Miremadi SR, Ashjaee M, Mahdavi Nejad A. Lithium-ion battery thermal management system with Al₂O₃/AgO/CuO nanofluids and phase change material. *Appl Therm Eng* 2020;180:115840. [\[CrossRef\]](#)
- [73] Wiriyasart S, Hommalee C, Sirikasemsuk S, Prurapark R, Naphon P. Thermal management system with nanofluids for electric vehicle battery cooling modules. *Case Stud Therm Eng* 2020;18:100583. [\[CrossRef\]](#)

- [74] Kiani M, Ansari M, Arshadi AA, Houshfar E, Ashjaee M. Hybrid thermal management of lithium-ion batteries using nanofluid, metal foam, and phase change material: an integrated numerical-experimental approach. *J Therm Anal Calorim* 2020;141:1703–1715. [\[CrossRef\]](#)
- [75] Zhou Z, Lv Y, Qu J, Sun Q, Grachev D. Performance evaluation of hybrid oscillating heat pipe with carbon nanotube nanofluids for electric vehicle battery cooling. *Appl Therm Eng* 2021;196:117300. [\[CrossRef\]](#)
- [76] Yetik O, Yilmaz N, Karakoc TH. Computational modeling of a lithium-ion battery thermal management system with Al₂O₃-based nanofluids. *Int J Energy Res* 2021;45:13851–13864. [\[CrossRef\]](#)
- [77] Kumar V, Singh SK, Kumar V, Jamshed W, Nisar KS. Thermal and thermo-hydraulic behaviour of alumina-graphene hybrid nanofluid in minichannel heat sink: An experimental study. *Int J Energy Res* 2021;45:20700–20714. [\[CrossRef\]](#)
- [78] Lyu Y, Siddique ARM, Majid SH, Biglarbegian M, Gadsden SA, Mahmud S. Electric vehicle battery thermal management system with thermoelectric cooling. *Energy Rep* 2019;5:822–827. [\[CrossRef\]](#)
- [79] Sirikasemsuk S, Wiriyasart S, Naphon P, Naphon N. Thermal cooling characteristics of Li-ion battery pack with thermoelectric ferrofluid cooling module. *Int J Energy Res* 2021;45:8824–8836. [\[CrossRef\]](#)
- [80] Li C, Li Y, Gao L, Garg A, Li W. Surrogate model-based heat dissipation optimization of air-cooling battery packs involving herringbone fins. *Int J Energy Res* 2021;45:8508–8523. [\[CrossRef\]](#)
- [81] Huang D, Zhang H, Wang X, Huang X, Dai H. Experimental investigations on the performance of mini-channel evaporator refrigeration system for thermal management of power batteries. *Int J Refrig* 2021;130:117–127. [\[CrossRef\]](#)
- [82] Zhao G, Wang X, Negnevitsky M, Zhang H. A review of air-cooling battery thermal management systems for electric and hybrid electric vehicles. *J Power Sources* 2021;501:230001. [\[CrossRef\]](#)
- [83] Yousefi T, Mousavi SA, Farahbakhsh B, Saghiri MZ. Experimental investigation on the performance of CPU coolers: Effect of heat pipe inclination angle and the use of nanofluids. *Microelectron Reliab* 2013;53:1954–1961. [\[CrossRef\]](#)
- [84] Arya A, Sarafraz MM, Shahmiri S, Madani SAH, Nikkhah V, Nakhjavani SM. Thermal performance analysis of a flat heat pipe working with carbon nanotube-water nanofluid for cooling of a high heat flux heater. *Heat Mass Transf* 2018;54:985–997. [\[CrossRef\]](#)
- [85] Aprianingsih N, Winarta A, Ariantara B, Putra N. Thermal performance of Pulsating Heat Pipe on Electric Motor as Cooling Application. *E3S Web Conf* 2018;67:1–6. [\[CrossRef\]](#)
- [86] Li X, Wang H, Luo B. The thermophysical properties and enhanced heat transfer performance of SiC-MWCNTs hybrid nanofluids for car radiator system. *Colloids Surfaces A Physicochem Eng Asp* 2021;612:125968. [\[CrossRef\]](#)
- [87] Vidhya R, Balakrishnan T, Kumar BS. Investigation on thermophysical properties and heat transfer performance of heat pipe charged with binary mixture based ZnO-MgO hybrid nanofluids. *Mater Today Proc* 2020;37:3423–3433. [\[CrossRef\]](#)
- [88] Xuan Z, Zhai Y, Ma M, Li Y, Wang H. Thermoeconomic performance and sensitivity analysis of ternary hybrid nanofluids. *J Mol Liq* 2021;323:114889. [\[CrossRef\]](#)
- [89] Ebrahim Qomi M, Sheikhzadeh GA, Fattahi A. Heat transfer enhancement in a microchannel using a pulsating MHD hybrid nanofluid flow. *Energy Sources Part A Recover Util Environ Eff* 2020;00:1–16. [\[CrossRef\]](#)
- [90] Bumataria RK, Chavda NK, Nalbandh AH. Performance evaluation of the cylindrical shaped heat pipe utilizing water-based CuO and ZnO hybrid nanofluids. *Energy Sources Part A Recover Util Environ Eff* 2020;00:1–16. [\[CrossRef\]](#)
- [91] Davin T, Pellé J, Harmand S, Yu R. Experimental study of oil cooling systems for electric motors. *Appl Therm Eng* 2015;75:1–13. [\[CrossRef\]](#)
- [92] Abdelsalam MY, Sarafraz P, Cotton JS, Lightstone MF. Heat transfer characteristics of a hybrid thermal energy storage tank with Phase Change Materials (PCMs) during indirect charging using isothermal coil heat exchanger. *Sol Energy* 2017;157:462–476. [\[CrossRef\]](#)
- [93] Galloni E, Parisi P, Marignetti F, Volpe G. CFD analyses of a radial fan for electric motor cooling. *Therm Sci Eng Prog* 2018;8:470–476. [\[CrossRef\]](#)
- [94] Alam MW, Bhattacharyya S, Souayah B, Dey K, Hammami F, Rahimi-Gorji M, et al. CPU heat sink cooling by triangular shape micro-pin-fin: Numerical study. *Int Commun Heat Mass Transf* 2020;112:104455. [\[CrossRef\]](#)
- [95] Belarbi AA, Beriache M, Che Sidik NA, Mamat R. Experimental investigation on controlled cooling by coupling of thermoelectric and an air impinging jet for CPU. *Heat Transf* 2021;50:2242–2258. [\[CrossRef\]](#)
- [96] Abdulmunem AR, Jalil JM. Indoor investigation and numerical analysis of PV cells temperature regulation using coupled PCM/Fins. *Int J Heat Technol* 2018;36:1212–1222. [\[CrossRef\]](#)
- [97] Pandey B, Banerjee R, Sharma A. Coupled EnergyPlus and CFD analysis of PCM for thermal management of buildings. *Energy Build* 2021;231:1–20. [\[CrossRef\]](#)
- [98] Kurhade A, Talele V, Venkateswara Rao T, Chandak A, Mathew VK. Computational study of PCM cooling for electronic circuit of smart-phone. *Mater Today Proc* 2021;47:3171–3176. [\[CrossRef\]](#)

- [99] Talele V, Thorat P, Gokhale YP, VK M. Phase change material based passive battery thermal management system to predict delay effect. *J Energy Storage* 2021;44:1–9. [\[CrossRef\]](#)
- [100] Peng L, Ni Z, Huang X. Review on the fire safety of exterior wall claddings in high-rise buildings in China. *Procedia Eng* 2013;62:663–670. [\[CrossRef\]](#)
- [101] Abdelatif MA, Zamel AA, Ahmed SA. Elliptic tube free convection augmentation: An experimental and ANN numerical approach. *Int Commun Heat Mass Transf* 2019;108:104296. [\[CrossRef\]](#)
- [102] Abdelatif MA, Omara MA. Free convection experimental study inside square tube with inner roughened surface at various inclination angles. *Int J Therm Sci* 2019;144:11–20. [\[CrossRef\]](#)
- [103] Abdelfattah AA, Ibrahim EZ, Sayed Ahmed SAE, Elwan WM, Elsayed ML, Abdelatif MA. Thermal performance augmentation of a semi-circular cylinder in crossflow using longitudinal fins. *Int Comm Heat Mass Transf* 2021;125:105159. [\[CrossRef\]](#)
- [104] Jadeja K, Bumataria R, Chavda N. Nanofluid as a coolant in internal combustion engine-a review. *Int J Ambient Energy* 2022;43:1–20. [\[CrossRef\]](#)
- [105] Katiyar A, Gupta NK. Effect of different aluminium oxide based nanofluid concentrations on the efficiency of solar water desalination system. *J Therm Eng* 2023;9:61–68. [\[CrossRef\]](#)
- [106] Karmveer, Gupta NK, Alam T, Cozzolino R, Bella G. A Descriptive review to access the most suitable rib's configuration of roughness for the maximum performance of solar air heater. *Energies* 2022;15:2800. [\[CrossRef\]](#)
- [107] Rathore PKS, Gupta NK, Yadav D, Shukla SK. Thermal performance of the building envelope integrated with phase change material for thermal energy storage: an updated review. *Sustain Cities Soc* 2022;79:103690. [\[CrossRef\]](#)